

---

# Biophysics and Molecular Biology of Cardiac Ion Channels for the Safety Pharmacologist

Michael K. Pugsley, Michael J. Curtis, and Eric S. Hayes

## Contents

1	Current Cardiovascular Safety Pharmacology Studies .....	151
1.1	Ion Channel Blockade Assays .....	151
1.2	QT as a Surrogate Biomarker and Studies Used to Assess Ion Channel Modulation .....	152
1.3	The Comprehensive In Vitro Proarrhythmia Assay .....	156
2	Myocardial Cell Types and Myocyte Coupling in the Heart .....	159
3	Bioelectrical Properties in the Myocardium .....	160
3.1	The Nernst Equation for Membrane Potential .....	160
4	Voltage-Gated Ion Channels and Genesis of Cardiac APs .....	163
4.1	Hodgkin–Huxley Equations .....	163
4.2	Genesis of the Cardiac AP .....	164
5	The Cardiac Sodium Channel .....	167
5.1	Molecular and Pharmacological Properties .....	168
6	Cardiac Calcium Channels .....	173
6.1	Molecular and Pharmacological Properties .....	173
7	Cardiac Potassium Channels .....	176
7.1	Diversity of Voltage-Gated Potassium Channels .....	176
7.2	Voltage-Dependent ( $K_V$ ) Transient Outward ( $I_{to}$ ) and Delayed Rectifier ( $I_K$ ) Channels .....	181
7.3	The Inward Rectifier Potassium Current ( $I_{Kir}$ ) .....	187
8	The Electrocardiogram .....	191
8.1	ECG Changes that Can Occur in the Myocardium .....	193
8.2	Early Afterdepolarisations .....	195

---

M.K. Pugsley (✉)

Global Safety Pharmacology and Toxicology/Pathology, Janssen Pharmaceuticals LLC, 1000  
Route 202 South, Raritan, NJ 08869, USA  
e-mail: [mkpugsley@yahoo.com](mailto:mkpugsley@yahoo.com)

M.J. Curtis

Cardiovascular Division, Faculty of Life Sciences & Medicine, King's College London,  
Rayne Institute, St Thomas' Hospital, London, UK

E.S. Hayes

Porolt, 3055 NW 57th Street, Seattle, WA 98107, USA

© Springer-Verlag Berlin Heidelberg 2015

M.K. Pugsley, M.J. Curtis (eds.), *Principles of Safety Pharmacology*, Handbook of  
Experimental Pharmacology 229, DOI 10.1007/978-3-662-46943-9\_7

149

8.3	Delayed Afterdepolarisations (DADs) .....	195
8.4	Re-entrant Arrhythmia Pathways .....	196
9	Conclusion .....	197
	References .....	197

## Abstract

Cardiac safety pharmacology is a continuously evolving discipline that uses the basic principles of pharmacology in a regulatory-driven process to generate data to inform risk/benefit assessment of a new chemical entity (NCE). The aim of *cardiac* safety pharmacology is to characterise the pharmacodynamic/pharmacokinetic (PK/PD) relationship of a drug's adverse effects on the heart using continuously evolving methodology. Unlike Toxicology, safety pharmacology includes within its remit a regulatory requirement to predict the risk of rare cardiotoxic (potentially lethal) events such as torsades de pointes (TdP), which is statistically associated with drug-induced changes in the QT interval of the ECG due to blockade of  $I_{Kr}$  or  $K_v11.1$  current encoded by hERG. This gives safety pharmacology its unique character. The key issues for the safety pharmacology assessment of a drug on the heart are detection of an adverse effect liability, projection of the data into safety margin calculation and clinical safety monitoring. This chapter will briefly review the current cardiac safety pharmacology paradigm outlined in the ICH S7A and ICH S7B guidance documents and the non-clinical models and methods used in the evaluation of new chemical entities in order to define the integrated risk assessment for submission to regulatory authorities. An overview of how the present cardiac paradigm was developed will be discussed, explaining how it was based upon marketing authorisation withdrawal of many non-cardiovascular compounds due to unanticipated proarrhythmic effects. The role of related biomarkers (of cardiac repolarisation, e.g. prolongation of the QT interval of the ECG) will be considered. We will also provide an overview of the 'non-hERG-centric' concepts utilised in the evolving comprehensive in vitro proarrhythmia assay (CIPA) that details conduct of the proposed ion channel battery test, use of human stem cells and application of in silico models to early cardiac safety assessment. The summary of our current understanding of the triggers of TdP will include the interplay between action potential (AP) prolongation, early and delayed afterdepolarisation and substrates for re-entry arrhythmias.

## Keywords

Activation • Atrial preparation • Biophysics • Calcium channel • Cardiac action potential • Channel kinetics • Comprehensive in vitro proarrhythmia assay • Delayed rectifier • Early afterdepolarisation • ECG • Hodgkin–Huxley • ICHS7A • ICHS7B • In silico modelling • Inactivation • Inward rectifier • Langendorff heart • Purkinje fibre • Safety assessment • Sodium channel • Stem cells

## 1 Current Cardiovascular Safety Pharmacology Studies

### 1.1 Ion Channel Blockade Assays

Each NCE is evaluated for potential proarrhythmic liability (particularly TdP liability) initially by evaluating potential adverse effects on cardiac ion channels in the very early stages of drug development. These ‘frontloading’ safety pharmacology (SP) studies are normally undertaken *before* selection of a candidate drug for development and before regulatory studies are conducted. Frontloading studies are conducted by 80 % of all companies. The safety pharmacologist is the individual primarily responsible for initiating, driving and leading the early SP assessment. Although there is increasing focus on a wide range of ion channels, all cardiac safety includes high-throughput (HT) evaluation of effects on the hERG-encoded  $I_{Kr}$  current (often abbreviated as hERG screening). The assay predominantly uses the cloned human channel expressed in either CHO or HEK cell lines (isolated myocytes are rarely used) as their primary test system. These studies are conducted at room temperature or at physiological temperatures (~37 °C). Temperature has an effect on channel kinetics; thus, physiological temperatures are recommended (Kirsch et al. 2004).

Larger companies require mandatory hERG screening prior to compound progression. Smaller companies may sell on their intellectual property (IP) rather than invest in a full SP programme. The following methodologies are used: automated patch clamp, non-automated patch clamp, ligand binding studies, and rubidium efflux studies. Selectivity screen/receptor binding profiling of the NCE is often undertaken. Other studies that are frontloaded include cardiac AP duration (APD) measurement in rabbit guinea pig and dog and haemodynamic/ECG studies in dogs or rodents (Lindgren et al. 2008).

Subsequently, either additional ion channel studies or more sophisticated voltage-clamp methods may be used in conjunction with *in vitro* APD studies to assess proarrhythmia liability. *In vivo* models may be used before selection of the candidate drug, but use is limited due to their low-throughput nature. Prior to first in human (FIH) studies *in vitro* APD and *in vivo* APD and QT interval assessments are usually undertaken to complement the early cardiac screening data, thus establishing a dataset used to inform an integrated risk assessment as described in the ICH S7A and ICH S7B guidelines (Anon. 2001, 2005). Almost no non-clinical safety work is conducted after FIH.

In summary, a large range of *in vitro* and *in vivo* cardiovascular (CV) studies are used by safety pharmacologists in order to fully characterise the safety profile of a lead candidate molecule.

## 1.2 QT as a Surrogate Biomarker and Studies Used to Assess Ion Channel Modulation

The cardiovascular safety core battery of tests evolved over many years due to the inherent difficulty in reaching consensus about how to safely test for risk of a rare but potentially lethal drug-induced cardiac syndrome known as TdP. Non-clinical detection of a clinically rare adverse event is difficult to undertake if the adverse event is equally rare in animals. Since this is the case for drug-induced TdP, a surrogate biomarker was needed. However, as surrogate biomarkers for rare events are difficult to validate (where validation requires the accumulation of a large database of positive and negative controls) and there is uncertainty over the extent of the risk that clinically established drugs have for generating the adverse effect in patients (no 'gold standard' or quantitatively structured template of human response to drugs), then reliable validation of the biomarker becomes an elusive (if not impossible) goal. This summarises the situation with TdP risk assessment. Today, a uniform international consensus exists regarding mandatory cardiovascular safety testing methods, which is, predictably, conservative and exhaustive: ICH guidelines S7A and S7B.

Since the 1970s, there has been a growing awareness that widening of the QT interval of the ECG is statistically associated with a risk in development of drug-induced TdP (Malik and Camm 2001; Shah 2001). This was initially recognised only for 'cardiovascular-targeted' therapeutic drugs such as prenylamine, bepridil, sotalol and quinidine (Vos 2001). However, it was then found that 'non-cardiovascular'-targeted drugs could also precipitate TdP and that this appeared to be most common among drugs that also widened QT interval (DePonti et al. 2002). In the 1990s, many well-known drugs were withdrawn from the market as a result of TdP liability, including terfenadine and astemizole (second-generation antihistamines), cisapride (a prokinetic GI agent with cholinomimetic and 5-HT<sub>4</sub> receptor agonistic properties), terodiline (an anticholinergic/antispasmodic drug effective in the treatment of urinary incontinence) and grepafloxacin (a fluoroquinolone antibiotic) (DePonti et al. 2002). This precipitated the collaboration between pharmaceutical companies and regulatory authorities that led to the construction of the guidance documents we now know as ICH S7A and S7B.

When the S7A guidance was published, selecting a method for evaluating TdP liability was an issue that was not addressed. Ventricular repolarisation delay is generally regarded as the best, albeit still poor, biomarker for TdP risk. A degree of consensus with respect to approach has been achieved, albeit through compromise regarding what actually constitutes a threshold transgression (in terms of magnitude of threshold dose and magnitude of threshold effect) for different putative TdP biomarkers such as prolongation of the QT interval and blockade of the cardiac potassium current  $I_{Kr}$  (Cavero and Crumb 2005). Despite the years since implementation of the SP guidance documents, there is still no agreement regarding the identification of a single best preclinical animal model for detection of TdP liability, and instead the compromise has been adoption of an integrated risk assessment strategy (Pugsley et al. 2008).

Cardiac SP *in vivo* methods primarily use conscious telemetered animals to assess the effects of the test item on the cardiovascular system. Variables that are recorded in the dog include blood pressure, heart rate and ECG (see Authier et al. 2015). Complementary studies, usually non-GLP in nature, include a number of *in vitro* assays that have been well characterised with utility in the safety profiling of an NCE. These assays include assessment of drug effects in the isolated guinea pig right atrium preparation, rabbit Purkinje fibre preparation, the isolated Langendorff heart and the isolated wedge preparation. Each assay will be briefly discussed.

### 1.2.1 The Isolated Atrial Preparation

The types of isolated tissues that can be used to assess drug effects on the heart are extensive and remain a cornerstone of not only the physiological and pharmacological evaluation of natural and synthetic drugs but also proved a means by which to characterise cardiac safety. The cardiovascular system is a rich source of tissue for *in vitro* studies. Some of the earliest assessments of a drug effect (i.e. not simply a CEREP non-functional binding study) can be made in isolated cardiac tissues, such as the isolated atrium. Such preparations can involve strips of atrial tissue (such as from the rabbit) or the entire atria (left and right) but usually just involve the single right atrium. Intact preparations are particularly useful in assessing the nature of a drug on cardiac function in terms of changes to beating rate, force of contraction, membrane potential as well as determining biochemical activity. Recently, Goineau et al. (2012) compared the sensitivity of three SP models that could be used in the assessment of drug-induced effects on cardiac conduction. They observed that rabbit atria were more sensitive at detecting lidocaine-induced cardiac slowing than rabbit Purkinje fibres or guinea pig atria.

Anatomically, in adult mammals, the right atrium is primarily used as it is larger than the left atrium and contains the anatomical structures necessary for cardiac conduction and the coronary circulation. Additionally, the right atrium spontaneously beats at a rate dominated by the sinus node and because atrial cells contain numerous G-protein-coupled receptors (GPCR) and ion channels provide a ‘multiple target’ testing assay. However, delineation of the mechanism of action for the drug effect is not easy to establish and would require follow-up studies. The strength of the assay is that it can be used as an early safety screen to direct medicinal chemistry synthesis of compounds that lack untoward cardiac effects. Moreover, drugs can be added directly to an organ bath, and there is no requirement for technically difficult aortic cannulation (required for the Langendorff model—see later) and so the technique maybe applies with ease to mouse models, in which gene modification studies are most conveniently undertaken. This allows for heritable risk to be factored into assessment.

### 1.2.2 The Isolated Purkinje Fibre

Cardiac Purkinje fibres are subendocardially located within the heart along the inner ventricular wall and are responsible for the spread of myocardial electrical activity that results in the generation of the QRS complex of the ECG. These fibres, first described by the Czech physiologist and anatomist Johannes (Jan) Evangeline

Purkinje (Purkyně) in 1839, are comprised of specialised cardiomyocytes with a distinctive ion channel profile that effect rapid conduction of an electrical impulse ( $\sim 4.0$  m/s) from the bundle branches through the heart to the working myocardium the point of termination of the cardiac conduction system (Sedmera and Gourdie 2014). It is the fast conduction in the Purkinje fibre that establishes the cardiac conduction synchrony of the ventricles from apex to base that maintains a consistent heart rhythm. However, it is this same property of these fibres that can make the heart susceptible to, or perpetuate, the development of re-entrant arrhythmias and abnormal automaticity (Boyden et al. 2010). Purkinje fibres are large cells with limited contractile elements and fewer mitochondria and conduction does not respond to changes in autonomic tone compared with cells of the working myocardium (Boyden et al. 2010). In SP the assay may consist of Purkinje fibres isolated from the rabbit, guinea pig or dog and usually involves determining the concentration–response profile and rate dependence of the NCE on AP parameters. These standard parameters include the AP amplitude (APA), maximum rate of ventricular depolarisation ( $V_{\max}$ ) and APD at 60 % and 90 % repolarisation (APD<sub>60</sub> and APD<sub>90</sub>). Additionally the magnitude of the effects of the NCE should be routinely compared to vehicle and usually a positive control (such as sotalol) conducted in parallel within the study.

SP studies have shown that isolated rabbit Purkinje fibres, when used in the assay, are highly sensitive to drugs with a greater propensity to prolong the APD and elicit early afterdepolarisations (EAD) compared to fibres from guinea pig, dog or swine (Lu et al. 2000, 2001). Thus, it appears that it is a highly specific and sensitive model to investigate drug-induced TdP liability. Lu et al. (2008) have also shown that there are marked differences in tissue response to drugs when isolated rabbit Purkinje fibres are used in the assay compared to either papillary muscle with ventricular trabeculae. Over the years, the assay has been well validated through the testing of many reference compounds (see Champeroux et al. 2005; Hanson et al. 2006; Aubert et al. 2006; Puddu et al. 2011) for use in the early de-risking stages of development (as a non-GLP assay) or as a component of the GLP-compliant in vitro core battery testing scheme. It has been identified as an important non-clinical assay in drug safety assessment by global regulatory authorities (Corrias et al. 2011).

### 1.2.3 The Langendorff Isolated Heart

The perfused isolated heart has many advantages in the study of the actions of an NCE on the mechanical (i.e. inotropic and lusitropic effects) and electrical properties of the heart (Bell et al. 2011; Clements-Jewery and Curtis 2014). The isolated heart was first described by Langendorff in 1895 as a simple preparation with which to study the activities of drugs. Briefly, hearts are perfused through the aorta with an oxygenated physiological buffer solution using a methodology essentially unchanged since originally described. The isolated heart is free of extrinsic nerves (but does contain a rich intrinsic innervation of ganglionic plexuses; see Brack 2014) and circulating systemic hormonal factors as well as variation in haemodynamics that may alter drug activities. A constant perfusion pressure closes

the aortic valve facilitating coronary artery blood vessel perfusion. The highly vascularised cardiac muscle ensures that exposure to drugs carried within the buffer rapidly gains access to all myocytes providing a sensitive measure of drug effects on contractility (mechanics), coronary flow and the electrocardiogram (ECG). This model is used extensively in SP studies (Lawrence et al. 2006; Guo et al. 2009) and is widely recognised as a surrogate for the study of human cardiac function and considered a conduit between *in vitro* cellular studies (hERG) and *in vivo* (conscious dog) screening methods. The nature of the preparation allows for hearts from a wide range of non-clinical species to be studied and may better predict effects observed *in vivo* than single cell studies since the syncytium is intact (Clements-Jewery and Curtis 2014). The rabbit and guinea pig hearts are used extensively in drug safety assessment since they show comparable electrophysiological responses to that observed in human hearts when similar drugs are investigated (Hondegheem and Hoffmann 2003; Hamlin et al. 2004). Thus, the Langendorff isolated heart provides a means by which to assess the safety profile of NCEs contiguously on electrical, mechanical and biochemical properties of the heart (Clements-Jewery and Curtis 2014; Curtis 1998).

#### 1.2.4 The Isolated Coronary-Perfused Wedge Preparation

The isolated coronary-perfused wedge preparation is a commonly used non-clinical model in SP (Lee et al. 2010) that was developed by Yan and Antzelevitch (1996). The preparation is highly sensitive to detect effects of drugs while remaining selective enough to differentiate between drugs with known TdP liability drugs and non-arrhythmic drugs (Wang et al. 2008). Because of the nature of the preparation, the NCE can be continuously infused into the perfusion medium at increasing concentrations and a number of superimposed physiological alterations such as hypokalaemia, bradycardia or tachycardia (albeit limited in duration to ~60 s in order to avoid myocardial ischaemia) can be assessed. This method makes use of the marked regional differences in electrophysiology across the ventricle (intramural dispersion) that is characteristic of the preparation. Drug effects are evaluated on three distinct tissues within the ventricle: the epicardium, mid-myocardium (M-cells) and endocardium (Yan et al. 1998). The M-cells are the last to complete repolarisation and this is thought to be due to the presence of a smaller, slowly activating, delayed rectifier current (IKs), a larger late depolarising sodium current (or late INa) and a larger electrogenic sodium–calcium exchange current (Yan and Antzelevitch 1998; Antzelevitch and Shimizu 2002). The model uses electrodes that are placed at the level of each tissue region, which then record the three transmembrane potentials simultaneously, with an accompanying ECG for reference. In addition to the standard ECG measures, transmural dispersion of repolarisation (TDR) can be evaluated as the ratio of the interval between the peak and end of the T-wave and the QT interval  $[(T_p - T_e)/QT]$  (Liu et al. 2006). The model also detects Phase 2 EADs and EAD-mediated R-on-T extrasystoles and an arrhythmia score can be applied for a semi-quantitative estimate of TdP potential.

The wedge preparation has been criticised on the grounds that transmural dispersion of the magnitude expressed is not found in an intact heart in which cell coupling largely precludes it (Curtis et al. 2013). However, this is not relevant if the model accurately predicts TdP liability with precision and accuracy. Indeed clinical relevance in the context of SP must be and need only be measured in terms of predictivity, and not the degree of identity between screen readout and human physiology.

While the isolated coronary artery-perfused ventricular wedge preparations have been shown to have a high specificity and selectivity for human torsadogens (Antzelevitch 2004; Liu et al. 2006), perceived limitations include the in vitro setting, the requirement for technical expertise and familiarity and the consequence that the model is not fit for high-throughput SP.

### 1.3 The Comprehensive In Vitro Proarrhythmia Assay

The clinical thorough QT (TQT) study (as outlined in the ICH E14 guidance) in conjunction with the series of non-clinical studies focused on assessing hERG current block (as outlined in the ICH S7B guidance) has effectively reduced the risk of developing (and subsequently approving) new drugs with the potential for precipitating torsades de pointes (TdP) cardiac arrhythmias. However, development and current conduct of this paradigm have come at a high cost to both the pharmaceutical industry in terms of the actual added cost to develop new drugs (i.e. conduct of the TQT study is ~\$4M/study) and society in terms of the loss to patients of potentially novel, effective drugs that have a hERG liability (or potential to prolong the QT interval) but with a low potential for proarrhythmia.

A novel cardiovascular risk assessment paradigm is being developed that would help to obviate conduct of the clinical TQT study (Darpo et al. 2014). The proposed Comprehensive In vitro Proarrhythmia Assay (CIPA) paradigm aims to modernise and provision current non-clinical, 'hERG-centric' cardiac safety screening efforts (Sager et al. 2014). A number of challenges and opportunities exist that are associated with adoption of a new approach in the evaluation of the arrhythmia potential of new drugs using novel in vitro (human stem cells) and in silico (cardiac AP modelling) methods and their application to clinically relevant arrhythmias such as TdP.

#### 1.3.1 Stem Cells and CIPA

Current alternative screening models and methods under consideration by the SP and regulatory communities for the CIPA initiative include stem cells in which hERG ( $I_{Kr}$ ) as well as other cardiac ion channels such as sodium (SCN5A), calcium (Cav1.2) and some potassium channels ( $I_{K1}$  and  $I_{Ks}$ ) can be assessed in totality (Pugsley et al. 2014). Rather than examining human ion channel isoforms heterogeneously expressed in cell lines (such as CHO or HEK) as is current practice in drug safety or, on the rare occasion, actually using isolated human cardiac myocytes, the community is investigating applicability of human-induced



pluripotent stem cells (Vidarsson et al. 2010; Peng et al. 2010). The undifferentiated human stem cell of embryonic origin (hESC) and induced pluripotent stem cell (iPSCs) of somatic origin (the latter with the potential advantage that they can be obtained from diseased patients, e.g. congenital LQTS) continue to be evaluated for all aspects of their cardiac electrophysiological potential (Tanaka et al. 2009). The use of stems cells, despite being an evolving technology, may have implications in SP testing related to the CIPA initiative. It has been suggested that the use of human stem cells would be desired in order to assess drug effects on cardiac ion channels, rather than using heterologous expression systems. These cells would be an alternative model to the use of isolated human cardiac myocytes which have been plagued with numerous limitations for many years. Thus, primary induced pluripotent cardiac stem cell (iPSC-CM) of somatic origin would be preferred for use compared to undifferentiated human stem cells of embryonic origin (hESC). Embryonic stem cells clearly have limitations that undermine their place in non-clinical research. However, primary iPSC-CM are being evaluated for cardiac electrophysiological properties and potential for use as a drug screening assay (Tanaka et al. 2009; Peng et al. 2010; Vidarsson et al. 2010; Gibson et al. 2014). Human iPSC-CM have the additional potential advantage that they can be obtained from diseased patients, e.g. with congenital LQTS. Intracellular recordings from individual cells (Peng et al. 2010) and multi-electrode arrays (MEA) enable measurement of sodium (SCN5A), calcium (Cav1.2) and potassium ( $I_{Kr}$  or hERG) current.

Implementation in CIPA will provide the impetus for conduct of ion channel blockade validation studies using stem cell technologies in order to establish a case for their use as an early drug screening assay or cardiovascular SP study model (with the hope they may be used routinely in the future as part of the core battery cardiovascular studies). However, not until phenotypic consistency, ion channel expression and electrophysiology profiles and responses to control drugs are established in terms of sensitivity, specificity and predictive utility are shown to be favourable versus current, established non-clinical models will stem cells transcend their status as secondary or tertiary cardiovascular assays. High-throughput screening (HTS) methods involving the use of stem cells create additional experimental concerns compared to those involving standardised CHO or HEK cell lines. A major constraint, in the foreseeable future, for the use of stem cells is their availability for HTS applications because of the number of cells required in automated chip-based patch-clamp systems. It should be remembered that a cell does not provide a complete physiological response.

### 1.3.2 In Silico Methods with Application to SP

For many years, there has been an ongoing effort to mathematically describe the cardiac AP (see below). Primarily driven by academic research groups, there has been a recent shift involving the integration of these researchers with those in industry in order to apply in silico methods to the CIPA initiative. For example, Mirams et al. (2014) characterised ion channel blockade for the series of ion channels that are responsible for genesis of the cardiac AP and proposed CIPA

candidates. These include hERG, the L-type calcium channel, the inward sodium channel, the KCNQ1/MinK or  $K_{v7.1}$  ( $K_{vLQT1}$ ) and transient outward K current). Mirams et al. (2014) used two standard high-throughput screening (HTS) assay systems to generate the data employed in the *in silico* models to simulate drug-mediated effects on human ventricular APs. Several mathematical simulation models were tested including the ten Tusscher and Panfilov (2006), Grandi et al. (2010) and O'Hara et al. (2011) models. Data derived from these *in silico* concentration–response simulations were compared to clinical QT results for the 34 compounds tested. At the study conditions used (1 Hz pacing and channel block determined at steady state) simulations tended to underestimate the QT prolongation observed in the clinic. Note that there are some differences, albeit subtle, between the numerous *in silico* methods utilised in AP simulation.

ten Tusscher and Panfilov (2006) developed a model of the cardiac ventricular AP based upon the measurement of human APD restitution, extensive description of intracellular calcium dynamics and importance of sodium channel recovery dynamics. The latter is important in defining the occurrence of electrical instability. Grandi et al. (2010) developed a mathematical model of the ventricular AP that characterised calcium handling as well as ionic currents measured in human cells. In development of their model they simulated basic excitation–contraction coupling phenomena and applied repolarising potassium current densities derived from a previously established rabbit myocyte model. However, unlike other models this one includes subsarcolemmal compartments where ion channels are programmed to ‘sense’ higher levels of calcium compared to the cytosol. In addition, transmural gradients for Ca handling proteins and the Na pump were simulated and both the rapid and slow inactivating components of the transient outward K current ( $I_{to}$ ) were simulated to differentiate between localisation either endocardially or epicardially. O'Hara et al. (2011) developed a human ventricular cardiac AP model based upon data measured from over 100 undiseased human hearts. Components of the model were evaluated over the human range of physiological frequencies and include calcium versus voltage-dependent inactivation of L-type calcium current ( $I_{CaL}$ ) and kinetics for the transient outward, rapid delayed rectifier ( $I_{Kr}$ ) and inward rectifier ( $I_{K1}$ ) potassium currents along with the  $Na^+/Ca^{2+}$  exchange pump ( $I_{NaCa}$ ). The authors also examined model response to rate dependence and restitution of cardiac AP duration (APD). Note that this model is referred to as the O'Hara-Rudy Dynamic (ORd) model.

The results derived from this ongoing research are important to development of the CIPA initiative currently ongoing between the pharmaceutical industry, contract research organisations and regulatory authorities (FDA) (Sager et al. 2014). The establishment of datasets of clinically used compounds should provide much needed information to the entire scientific community regarding adoption and applicability of *in silico* simulations in safety hazard identification as well as the nature of the data derived from HTS (vs. patch clamp) methods subsequently used in simulation methods.

Thus, application of *in silico* methods, with noted limitations, may have use in studies preceding frontloading SP cardiovascular studies provided that the

respective participants (companies or CRO laboratories) have the capability (i.e. informational technology computing capability, technical understanding of the mathematical models used in the model construction, etc.) to incorporate such assays into discovery screening procedures. Introduction could increase throughput and limit development of chemical scaffolds with potential cardiac liability.

The anticipated outcome from this change in paradigm is the development of a non-clinical, standardised in vitro assay that determines the effects of drugs on the major cardiac ion channels and provide an assessment of the potential to precipitate clinical proarrhythmia, obviate conduct of the clinical TQT study and facilitate more efficient drug discovery efforts. In order to understand the fundamentals of this novel paradigm, it is important to review fundamental cardiac electrophysiology including basic ion channel biophysics as well as review some fundamental cardiac arrhythmia mechanisms to achieve this alternate approach.

---

## 2 Myocardial Cell Types and Myocyte Coupling in the Heart

The safety pharmacologist, when conducting cardiac studies, should know that within the myocardium cardiac cells (myocytes) differ both in their morphology and electrophysiological properties. This distinction must be clearly appreciated since this cellular disparity exists between atrial and ventricular myocytes as well as transmurally within ventricular muscle. At least five distinct types of cell can be distinguished based upon anatomical, morphological and electrophysiological properties. These cell types are found in the sino-atrial node (SAN) tissue, atrial muscle, atrio-ventricular node (AVN) tissue, His-Purkinje fibres and ventricular muscle. In general these cells, usually quadrangular in shape (50–100  $\mu\text{m}$  in length by 10–20  $\mu\text{m}$  in width), though bounded in the usual way by their cell membranes (the sarcolemma) and separated from their neighbours by extracellular fluid, are also anchored to adjacent cells, mainly end to end, by adhesive complexes called intercalated discs.

The intercalated disc is composed of three structurally distinct regions: (a) the *macula adherens* or *desmosome* which is a complex where the central lamella appears to receive filamentous projections from the sarcolemma providing integrity to muscle during contraction, (b) the *fascia adherentes* or ‘intermediate junction’ where actin myofibrils terminate, and (c) the *nexus* or gap junction which provides a low impedance pathway permitting the conduction of APs from cell to cell.

These unique sites of cellular communication sanction the propagation of electrical impulses, and hence contraction, from their origin in SAN pacemaker cells to the ventricles. Thus, the heart functions as an electrical and mechanical syncytium in which the anatomical arrangement and diverse electrical properties of cells serve to produce the sequential cell activation that underlies the coordinated function of the heart.

### 3 Bioelectrical Properties in the Myocardium

The electrical properties of cardiac myocytes are best introduced and described in terms of circuit elements. These concepts are of relevance to understanding of drug–ion channel interactions and hence safety characterisation of a new chemical entity (NCE) or biological drug. Important components of these idealised circuits include conductors, capacitors and voltage generators (or batteries) (Hubbard et al. 1969). An understanding of how the cardiac AP (AP) is generated and propagated depends upon both knowledge as to how these elements are arranged in cells and their relation to electric current. Electrical *current* is simply defined as a flow of ions (of either positive or negative charge). By convention, current flows from a positive to a negative direction. Thus, cations (positive ions) such as  $K^+$  and  $Na^+$  flow in the same direction as current. The *potential* (or *voltage*) gradient is the force that causes charged particles to move. In a *conductor*, Ohm's law is followed such that  $I = GV$  or  $V = IR$  where  $R$ , resistance, is the inverse of conductance ( $G$ ) and  $V$  (voltage) is the potential difference between the points between which the current, ( $I$ ), flows. Thus, in a conductor (such as a myocardial cell membrane), there can be no voltage gradient unless there is current flow and no current flow unless there is a voltage gradient. Ionic (or salt) solutions are Ohmic. It is thought that these charged particles (ions) move in an electric field rapidly and thus reach a limiting velocity; the point at which 'frictional' forces balance the electrical force and current becomes proportional to the voltage gradient. The heart (not unlike the whole human body) can be thought of as a 'volume conductor', which can be simulated by a three-dimensional network of linked resistors. This simulation of the heart can result because myocardial cell membranes act as capacitors. While anisotropy, the non-uniform conductivity that depends upon current direction, is characteristic of many tissues (muscle in particular), it is especially important to the heart as it ensures proper uniform excitation of cardiac muscle and contraction (Pugsley and Quastel 1998).

*Capacitance* results whenever two conductors are separated by an insulator. In this case, a potential difference can be maintained indefinitely between the two conductors. Then, by definition,  $Q = CE$  and  $I = dQ/dt = CdE/dt$  where  $Q$  is charge and capacitance is  $C$ . When the voltage across a capacitor is altered charged particles move to or from both sides; this in effect results in a current 'through' the capacitor that is proportional to the rate of change of the voltage. Conversely, the voltage across a capacitor cannot change instantaneously; rather the charging or discharging of the capacitor is time dependent.

#### 3.1 The Nernst Equation for Membrane Potential

Electrophysiological studies show that most cells have an average resting membrane potential of  $-80$  mV. This value has been attributed to unequal concentrations across the membrane of ions to which the membrane is permeable. The myocardial cell can be thought of as being composed of two compartments

corresponding to the inside and outside of the cell. These compartments are separated by a membrane that is permeable to only one ion,  $K^+$  for example. Thus, inside the cell are  $K^+$  ions and the charge on these ions is balanced predominantly by large negatively charged (anionic) protein molecules which cannot penetrate through pores in the membrane. Outside the cell there is a relatively low concentration of  $K^+$  ions and other additional ions that cannot pass through the membrane. In order for this model to be effective, it is assumed that there is no potential across the membrane. More intracellular  $K^+$  ions, by thermal movement, leave the cell through the membrane pores than enter. Since the  $K^+$  ions move outward from the cell and are not accompanied by anions, the result is a net negative charge in the cell. This negative charge then opposes the exit and promotes the entry of  $K^+$ . It can be calculated that this exactly balances the tendency of  $K^+$  ions to flow from high to low concentration when the transmembrane potential is that given by the Nernst equation (Pugsley and Quastel 1998). Thus for any ion,  $J$ , with concentrations  $[J]_o$  outside and  $[J]_i$  inside, and valence  $z_j$  this equation states that  $E_J = RT/z_j F \cdot \ln ([J]_o/[J]_i)$  and for an ion such as  $K^+$  this equation can be written as  $E_K = RT/F \cdot \ln ([K^+]_o/[K^+]_i)$ . In these equations,  $R$  is the universal gas constant,  $T$  is the absolute temperature and  $F$  is the Faraday constant (96,500 C/mol).  $E_K$  is termed the ‘equilibrium potential’ or ‘reversal potential’ for  $K^+$  ions and it is the transmembrane voltage at which the net flow of  $K^+$  ions through the membrane is zero. In this hypothetical cell model, the concentration difference across the membrane results in a stable situation where transmembrane potential is maintained at  $E_K$  and  $[K^+]_i$  remains constant. Note that the myocardial cell membrane is permeable to a number of anions and cations, so each of the resulting derivations of the above equation must consider the valence of the ion in question. Thus for a membrane that is permeable to any of these ions, modifications can be made to the equation. For  $Na^+$  ions, the equation can be written as  $E_{Na} = RT/F \cdot \ln ([Na^+]_o/[Na^+]_i)$  while for  $Ca^{2+}$  ions  $E_{Ca} = RT/2F \cdot \ln ([Ca^{2+}]_o/[Ca^{2+}]_i)$  and for  $Cl^-$  ions  $E_{Cl} = -RT/F \cdot \ln ([Cl^-]_o/[Cl^-]_i)$  or  $E_{Cl} = RT/F \cdot \ln ([Cl^-]_i/[Cl^-]_o)$ .

For a cell membrane that has channels allowing permeation of more than one type of ion, the resting membrane potential will evidently result from a compromise between the equilibrium potentials for each of the various contributing ions. Two approaches can be used to calculate cell potentials. The first method calculates the theoretical current carried by each ion at various voltages. The Goldman–Hodgkin–Katz (GHK) current equation (Hille 1992) was developed based on the assumption that the electrical field in the membrane is constant. It states that for any ion  $J$  that  $I_J = P_J z_j F \cdot v_j \cdot ([J]_i \exp(v_j) - [J]_o) / (\exp(v_j) - 1)$  where  $v_j = V / (RT/z_j F)$ . In this equation,  $P_J$  is the membrane permeability to the  $J$  ion and  $V$  is the potential across the membrane. As a result, in this equation current is non-linearly related to voltage, i.e. the membrane becomes a non-Ohmic conductor, unless the ionic concentrations on the two sides of the membrane are equal. The GHK voltage equation (Hille 1992) can be easily acquired by determining the voltage at which the sum of all currents is zero. For a membrane that is permeable only to  $K^+$ ,  $Na^+$  and  $Cl^-$  and for which no other source of membrane current exists, the equilibrium or resting membrane potential,  $V_r$ , is  $V_r = (RT/F) \cdot \ln \{ (P_K [K^+]_o + P_{Na} [Na^+]_o + P_{Cl} [Cl^-]_i) /$

$(P_K[K^+]_i + P_{Na}[Na^+]_i + P_{Cl}[Cl^-]_o)$ . In fact, this equation can be correctly applied when the electrical field in the membrane is not uniform.

Physiologically, the  $Cl^-$  ion terms in these equations can often be ignored. With a high external  $Na^+$  and high internal  $K^+$ , the resultant  $V_r$  (whatever its value may happen to be between  $E_K$  and  $E_{Na}$ ) cannot be sufficiently negative to prevent the continuous egress of  $K^+$  ions and entry of  $Na^+$  ions. Therefore, stability of the cell becomes paramount and requires an active (and perpetual energy consuming) ionic transport mechanism. The ‘sodium/potassium pump exchanger’ then continuously extrudes  $Na^+$  ions and imports  $K^+$  ions.

The second approach in the derivation of the resting membrane potential of a cell considers the equivalent circuit of the membrane. With a separation between the inside and outside of the cell, there develops a capacitance and voltage potential, with an internal resistance (or conductance) that corresponds to each of the relevant permeant ions. Simple mathematical equations can be developed for each ion such that for  $K^+$  ions  $I_K = g_K (V - E_K)$ , for  $Na^+$  ions  $I_{Na} = g_{Na} (V - E_{Na})$ , for  $Cl^-$  ions  $I_{Cl} = g_{Cl} (V - E_{Cl})$  and for  $Ca^{2+}$  ions  $I_{Ca} = g_{Ca} (V - E_{Ca})$ . As with the GHK equations for the ‘resting’ state of membrane currents, the sum of all currents is zero and the equation becomes  $V_r = (g_K E_K + g_{Na} E_{Na} + g_{Cl} E_{Cl} + g_{Ca} E_{Ca}) / (g_K + g_{Na} + g_{Cl} + g_{Ca})$ . With this model, there is a continuous inward  $Na^+$  and  $Ca^{2+}$  current that is balanced by the sum of many outward  $K^+$  currents (see below for details on  $K^+$  current subtypes involved). However, unlike the GHK current equation, this approach does not account for the fact that, in general, conductance should be non-linear, i.e. it should depend upon voltage, since each ion exists in unequal concentrations on either side of the membrane. However, this equivalent circuit model can be applied if it is assumed that conductance is nearly a constant when associated with small changes in membrane potential and that, in myocytes, changes in the potential of the cardiac cell membrane are associated with *large* changes in conductance.

In an attempt to refine the above formulation, it was thought that perhaps it might be more accurate to describe the components of the equivalent circuit (i.e. the combination of battery and internal resistance) for each ion *channel* rather than to a particular ion. As well, to impart relevance to the system to accurately model the cardiac myocyte (as has been done by Noble & Mirams, O’Hara & Rudy and ten Tusscher & Panfilov amongst others), this approach should include as many different types of physiological ion channels as possible. Each voltage (or equilibrium potential) is represented not by the Nernst equation for a particular ion but rather by the GHK voltage equation using both ion concentrations and permeability ratio(s). This approach was formally described for currents in the mammalian ventricular cell by Luo and Rudy (1991) who used  $Na^+$  and  $Ca^{2+}$  currents, three distinct  $K^+$  currents as well as a ‘background’  $K^+$  current with an equilibrium potential between  $E_K$  and  $E_{Na}$ .

The equivalent circuit model of the membrane is best visualised schematically where capacitance represents the insulating myocardial lipid bilayer and each conductor–voltage (battery) combination represents a type of ionic channel.

Similarly for the more mathematically inclined, this may be a simple mathematical model such that the sum of all currents ( $CdV/dt$ ) must be zero.

The greatest physiological application for the equivalent circuit model is where myocardial cells are represented as a ‘ladder’ network. In the case of the heart, myocytes are represented as being connected end to end (which they are within the heart) with an internal resistance ( $R_i$ ) between two cells. Within the context of the heart, it must be realised that myocytes are connected to adjacent cells and therefore the network most accurately reflects the physiological scenario when considered in two or even three dimensions.

---

## 4 Voltage-Gated Ion Channels and Genesis of Cardiac APs

Our current understanding of electrical activity of cardiac muscle is based upon the observation that transmembrane potentials result from the coordinated integration of the opening and closing of many different ion channels. The corresponding changes in ionic permeability and conductance result in the flow of current, genesis of an AP and contraction of heart muscle.

Development of the theory of AP genesis and propagation in nerve and cardiac muscle resulted from the work of Hodgkin and Huxley (1952). APs in excitable cells result from the presence of voltage-gated ion channels that open and close depending upon the voltage across the membrane. Depolarisation of the resting membrane potential causes the opening of voltage-gated  $\text{Na}^+$  channels. This increase in  $\text{Na}^+$  permeability (or conductance,  $g_{\text{Na}}$  or  $G_{\text{Na}}$ ) results in the development of an inward current which enhances depolarisation and increases  $g_{\text{Na}}$ . This, in turn, further increases the inward current and  $g_{\text{Na}}$  until a maximum is attained. If this were the case, the membrane potential would be permanently shifted to  $E_{\text{Na}}$  in response to *any* depolarisation. Several factors prevent this event from transpiring. These include the fact that resting conductance allows for only a small increase in  $g_{\text{Na}}$  and inward current (which does not adversely affect the transmembrane potential), voltage-gated  $\text{Na}^+$  channels rapidly inactivate (within several milliseconds after depolarisation) and depolarisation marks the opening of voltage-gated  $\text{K}^+$  channels which shifts the membrane potential back to  $E_{\text{K}}$ . In contrast to nerves, the situation in the heart is complicated by the presence of voltage-gated  $\text{Ca}^{2+}$  channels. These channels mediate the ‘slow inward current’ ( $I_{\text{si}}$ ) that is predominantly responsible for the plateau phase of the AP (see details below). In some tissues, such as the sino-atrial and atrio-ventricular nodes, voltage-gated  $\text{Ca}^{2+}$  channels predominate and provide a basis for the AP.

### 4.1 Hodgkin–Huxley Equations

It was from studies and conclusions based upon the classical work of Hodgkin and Huxley (1952) that provides us with a basis for a mathematical description of voltage-dependent ion channel conductance. Their experimental strategy was

essentially to record electrical activity inside a giant squid axon cell using a 'voltage clamp'. Experimental evidence however did not support the predicted change in current amplitude. The theoretical model predicts that if conductance were constant, then steady current responses should result, and this was not observed. Rather, experimental currents were not maintained in a steady state. The initial inward  $\text{Na}^+$  current reached a maximum quickly but with time subsequently declined. An outward  $\text{K}^+$  current that slowly reached a maximum immediately followed decline in this current. Recordings of these currents at the given voltages that generated them allowed for a calculation of the conductance of each ion channel type involved in electrical activity in the axon. The fundamental feature observed for  $\text{K}^+$  ion channels was that with depolarisation the sigmoidal rising phase of the conductance curve for this ion could be mathematically defined as an exponential rise to a maximum. Potassium channel conductance could be expressed as  $g_{\text{K}} = G_{\text{K}} \cdot n^4$  where  $G_{\text{K}}$  is the maximal possible  $g_{\text{K}}$  and  $n$  is a parameter (usually less than 1.0) that changes according to the equation  $dn/dt = \alpha_n(1 - n) - \beta_n n$  or  $dn/dt + (\alpha_n + \beta_n)n = \alpha_n$  with both  $\alpha_n$  and  $\beta_n$  being a constant at any given transmembrane potential,  $V$ . Experimentally a change to a new constant voltage would allow for a new set of values for  $\alpha_n$  and  $\beta_n$ . These values are such that when the difference for  $n$  is determined for its final value, the path it follows is an exponential decrease in time course where the time constant,  $\tau_n$ , equals  $1/(\alpha_n + \beta_n)$ .

This mathematical formalisation for the experimentally obtained values allowed  $\alpha_n$  and  $\beta_n$  to be obtained for any given membrane potential. Thus, since  $n_f$  is given by the 4th root of the final  $g_{\text{K}}$  divided by maximum possible  $g_{\text{K}}$ , the resulting equations determined by Hodgkin and Huxley resembled those obtained by the GHK current equation. It was theorised that the set of obtained equations for  $\text{K}^+$  correspond to the gating or movement of 4 ' $n$ ' particles within the membrane and that the 'on' rate value for movement could be described by  $\alpha_n$  and the 'off' rate value by  $\beta_n$  (Hodgkin and Huxley 1952).

By using a similar recording approach and mathematical analysis profile for the rapidly activating and inactivating  $\text{Na}^+$  current, it was found that  $g_{\text{Na}}$  could be described by the equation  $g_{\text{Na}} = G_{\text{Na}} m^3 h$ . In this equation, the ' $m$ ' term describes the activation properties of the channel while the ' $h$ ' term describes the 'inactivation gate' the actions of which are governed by the time-independent parameters  $\alpha_m$  and  $\beta_m$  and  $\alpha_h$  and  $\beta_h$ , respectively. Mathematically (and experimentally) ' $m$ ' increased while ' $h$ ' decreased with membrane depolarisation. From their work, Hodgkin and Huxley showed that they could mathematically reconstruct the time course (and magnitude) of the squid axon AP.

## 4.2 Genesis of the Cardiac AP

The cardiac AP, illustrated in Fig. 1 for a ventricular myocyte, is conventionally composed of four phases. A rapid upstroke (phase 0) is followed by a brief peak (phase 1) followed by a sustained plateau (phase 2). A rapid repolarisation (phase 3) begins after several hundred milliseconds have elapsed and this is followed by



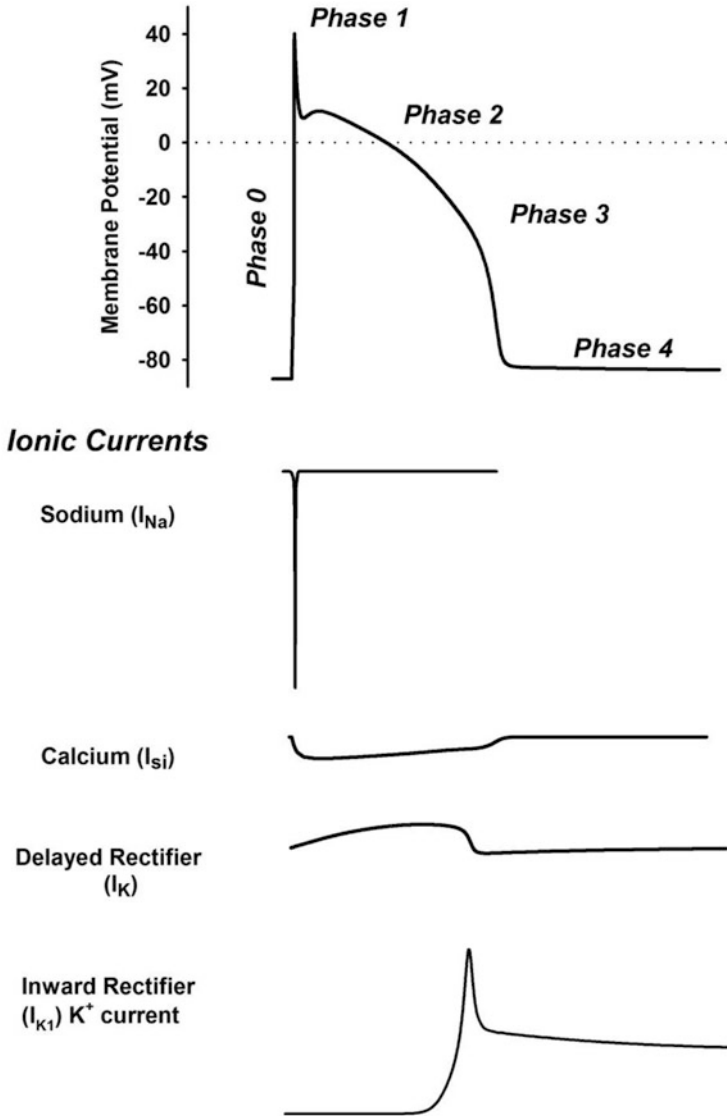


**Fig. 1** The cardiac action potential (AP) (*upper panel*) conventionally consists of several phases (0–4) with a duration of approximately 300 ms. Phase 0 corresponds to membrane depolarisation ( $Na^+$  influx), while phase 1 shows the early rapid repolarisation of the membrane. Phase 2 is the plateau of the AP (due to a reduction in  $Na^+$  influx and increase in  $Ca^{2+}$  influx), while phase 3 shows membrane repolarisation (resulting from the coordinated opening and closing of many different  $K^+$  channels). Phase 4 corresponds to the resting membrane potential. The *lower panels* depict the currents produced by the movement of several different ions across the membrane. By convention, both the inward  $Na^+$  ( $I_{Na}$ ) and  $Ca^{2+}$  ( $I_{Ca}$ ) ionic currents are shown downward. Several of the outward  $K^+$  ionic currents responsible for repolarisation are shown: the delayed rectifier ( $I_K$ ) and the inward rectifier ( $I_{K1}$ ). *Note that current amplitudes are not shown to scale*

phase 4 that persists until the next rapid upstroke event. Thus, the shape of the AP is governed by ionic current flux via gated channels in the membrane for sodium, calcium and potassium (Fig. 1). As well, membrane pumps and exchangers such as for Na/K-ATPase and Na/Ca are involved. The properties of the AP change moderately amongst tissue types. In pacemaker cells of the nodal tissues (and to a lesser degree in atrial cells and Purkinje fibres), phase 4 is characterised by a slow steady depolarisation from the resting membrane potential ( $V_m$ ) that leads to a 'threshold' potential (TP). When this potential is met, a rapid upstroke (phase 0) results and a nodal AP develops that is composed of similar 'phases' as in ventricular or other cardiac cells. While there may be some differences in regard to phase 4 development in various cardiac tissue, the fundamentals of AP generation remain essentially unchanged. The pacemaker current shapes the periodicity of oscillations in the heart since this current is activated by the hyperpolarised cell membrane at the conclusion of the AP.

The ventricular AP has been mathematically modelled by several groups of researchers (Hille 1992; DiFrancesco and Noble 1985). In each model, the genesis of the AP depends upon an accurate account of the biophysical and physiological properties of the component ionic currents. These properties are then integrated into a series of uniform equations (which are based upon those of Hodgkin and Huxley) and the AP model developed.

The inward, fast voltage-gated  $\text{Na}^+$  channel ( $g_{\text{Na}}$ ) is responsible for producing phase 0 and the rapid upstroke of the cardiac AP. It is best approximated by the equation  $g_{\text{Na}} = G_{\text{Na}} m^3 \cdot h \cdot j$ , where the  $j$  represents a slow inactivation gate component of the current which has its own voltage-dependent  $\alpha$  and  $\beta$  rate constants.

While  $\text{Na}^+$  channels rapidly inactivate as the membrane potential ( $V_m$ ) approaches the equilibrium potential (0 mV), a second voltage-gated ion channel is activated that is carried by  $\text{Ca}^{2+}$  ions. Calcium channels carry  $I_{\text{si}}$  that is responsible for the plateau phase of the AP (Fig. 1). These channels activate rapidly at approximately  $-40$  to  $-20$  mV and inactivate slowly. Calcium current can be approximated by the equation  $g_{\text{Ca}} = G_{\text{Ca}} \cdot d \cdot f$  where voltage-dependent rate constants ( $\alpha$  and  $\beta$ ) are determined for  $d$  and  $f$ . Many  $\text{Ca}^{2+}$  channel subtypes occur in the body. In the heart, at least 2 isoforms can be found: the 'L' and 'T' types (see below for details).

Within a short period of time ( $\approx 150$  ms), cardiac  $\text{Ca}^{2+}$  channels begin to inactivate and  $\text{K}^+$  channels begin to activate. Repolarisation becomes relatively rapid when the total outward  $\text{K}^+$  current becomes appreciably greater than inward  $\text{Ca}^{2+}$  current. A large number of voltage- and non-voltage-gated  $\text{K}^+$  currents are involved in repolarisation of the cardiac AP. The voltage-gated  $\text{K}^+$  currents include the transient outward  $\text{K}^+$  current ( $I_{\text{to}}$ ), one of the earliest channels to open (during phase 1) to begin repolarisation, the outward or delayed rectifier current ( $I_{\text{K}}$ ) which opens at the end of phase 2 and is the main  $\text{K}^+$  current responsible for ventricular repolarisation and the inward rectifier  $\text{K}^+$  current ( $I_{\text{K1}}$ ) which, unlike other  $\text{K}^+$  currents, closes during depolarisation and is responsible for maintenance of the resting membrane potential (see the lower panel of Fig. 1 for details).

An integration of the equations discussed above can accurately predict the shape of the AP. These equations can not only predict the shape of the AP but can be used to investigate changes in cellular physiology (such as elevated or reduced ion concentrations associated with disease states), the presence of 'unusual' electrical activity (such as is found with various arrhythmias resulting from myocardial ischaemia or infarction) or how drugs may interact with multiple ion channels concurrently and modulate or alter the AP.

In an actual heart, the situation is much more complicated than what can be described for a single isolated myocyte. Myocardial cells are coupled in three dimensions to adjacent cells as a means with which to assure the unified propagation of the AP and all cells assist in generating an AP synchronously. If this does not occur, disparity exists within the ventricle and altered excitability may result in disastrous consequences including proarrhythmia and sudden cardiac death. The uniform propagation of the AP is required for contractility and depends upon factors such as the geometric arrangement of cells, cell-to-cell coupling, the functional properties of each ion channel type involved in its genesis and current density within the cell membrane and its variation within regions of the heart.

---

## 5 The Cardiac Sodium Channel

Hodgkin and Huxley studied sodium conductance in the squid giant axon and were the first to propose a structural model for the channel such that the voltage-dependent opening and closing of membrane 'gates' resulted in a change in membrane permeability to sodium. The permeability change generated the AP and was responsible for the transmembrane movement of sodium ions. They proposed 'm' as an activation gate particle and 'h' as an inactivation gate particle, which display distinct kinetic properties highly dependent upon changes in membrane potential. Hodgkin and Huxley also postulated that for the conformational transitions of these gates to be voltage dependent, there must be a voltage sensor, or charge movement, during such transitions. They predicted the existence of the 'gating current'.

Depolarisation of the cell membrane opens  $\text{Na}^+$  channels. However, this event only occurs after some delay. During this short time period ( $<1$  ms), charge movement occurs. This delay was described as a series of voltage-dependent, closed-state conformational transitions the macromolecular protein which comprised the  $\text{Na}^+$  channel had to pass through before the channel opened. The cause of this delay remained elusive until 1973 when Armstrong and Bezanilla first recorded the 'gating current'. It was a current of small amplitude (0.13 pA) and fast kinetics (80  $\mu\text{s}$  to reach a maximum) (Armstrong and Bezanilla 1974). Thus, a majority of this current flows prior to the opening of the m gate for activation.

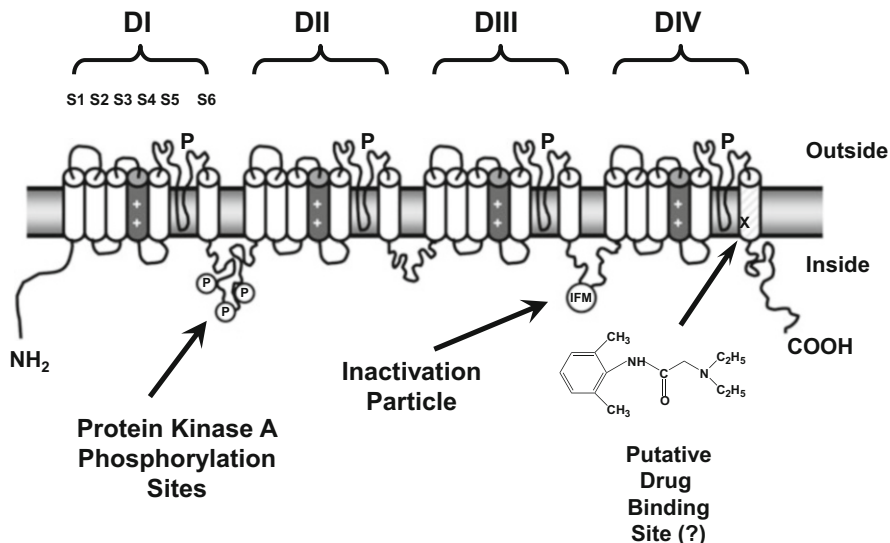


**Fig. 2** A schematic of the proposed molecular structure of the Na<sup>+</sup> channel present in the heart. This model depicts the transmembrane folding of the primary structure of the Na<sup>+</sup> channel α-subunit. The domains of the channel are indicated as DI–DIV. The six α-helical transmembrane-spanning sequences are indicated as S1–S6 for the DI domain. Some experimentally determined sites for protein kinase A phosphorylation and local anaesthetic binding are shown. Those sequences involved in channel inactivation are also indicated along with those regions that constitute the ion channel pore (P)

## 5.1 Molecular and Pharmacological Properties

Molecular studies have revealed characteristics of the Na<sup>+</sup> channel itself as well as the putative ‘voltage sensor’ for the gating current (see Fig. 2). All voltage-gated Na<sup>+</sup> channels are comprised of approximately 2,000 amino acids and contain four homologous internal repeats (DI–DIV), each of which has six putative transmembrane (S1–S6) segments (Catterall 1993; Denac et al. 2000). The α-subunit is a phosphorylated and glycosylated protein that forms the ion channel pore and contains a particular region, the fourth transmembrane segment, S4, which is composed of a number of positively charged amino acids (lysine and arginine) and has been postulated to be the voltage sensor (Catterall 1993). Displacement by the change in membrane potential of these amino acids may be responsible for the gating current (Catterall 1995). The outward gating charge for sodium is due to the movement of 6 charges across the membrane. This finding corroborated the proposed charge displacement equivalent to 6 electrons flowing from the extra- to intracellular side of the membrane by Hodgkin and Huxley (1952). However, despite the implication of the S4 region in gating, the mechanism by which activation is initiated is not completely elucidated but does immediately precede Na<sup>+</sup> channel opening. The S6 regions within each of the four domains of the α-

subunit are thought to form the pore region of the channel while the P loops from each domain (see Fig. 2 for details) comprise the 'selectivity' filter in the outer or more extracellular region of the pore (Catterall 2001). Sato et al. determined, at a resolution of 19 Å, the structure of the complete Na<sup>+</sup> channel in 2001. From a reconstruction of cryo-electron microscopic images, it is suggested that the Na<sup>+</sup> channel is bell shaped with the bulk of the protein structure (47 %) existing cytoplasmically. Structural features of the protein suggest an intercellular region for the inactivation particle and gating 'pores' for the outward movement associated with the voltage-sensing S4 transmembrane helices of each domain (Sato et al. 2001). These images also suggest that the central pore formed by the  $\alpha$ -subunit is not simply linear across the membrane as has been suggested for decades but rather is divided into four branches that connect the cytoplasm to the extracellular medium (Sato et al. 2001).

Most Na<sup>+</sup> channels are heterotrimeric complexes in the membrane. The  $\alpha$ -subunit ( $\approx$ 260 kDa) interacts with at least 2 small auxiliary  $\beta$ -subunit proteins. The  $\beta_1$ -subunit ( $\approx$ 36 kDa) is non-covalently associated with the  $\alpha$ -subunit and has been shown to increase Na<sup>+</sup> current amplitude and increase the kinetic rate of activation and inactivation of the channel (Isom et al. 1992). While the expression of the  $\alpha$ -subunit alone results in a functional channel, the  $\beta_1$ -subunit is responsible for refining the kinetic activity of the channel. These properties are crucial to the neuronal isoform of the channel but not the cardiac isoform of the channel. The  $\beta_2$ -subunit ( $\approx$ 33 kDa) modulates Na<sup>+</sup> channel localisation in tissue. Various subtypes of voltage-gated Na<sup>+</sup> channels have been described (see Table 1) (Goldin 2001). The cardiac subtype is distinguished from most by being relatively insensitive to blockade by the puffer fish neurotoxin, tetrodotoxin.

Initially, local anaesthetics and anticonvulsant and antiarrhythmic drugs were believed to interact with the Na<sup>+</sup> channel and immobilise a fraction of the gating charge when the channel was blocked. However, Hanck et al. (1994) showed that drugs could bind the cardiac channel gate, but with altered kinetics, i.e. exhibit a reduced voltage dependency. In light of the Modulated Receptor Hypothesis (see below), this may alter our perspectives regarding the mechanism by which drugs interact with the Na<sup>+</sup> channel. Thus drug occupancy may reduce the voltage dependence of gating by inhibition of voltage-sensitive charge movement rather than by drugs producing a shift in channel states to the favoured drug-bound inactive state of the channel (Hanck et al. 1994).

Activation (or gating) is a change between a closed and resting (non-conducting) state of the Na<sup>+</sup> channel to an open (conducting) state in response to a change in membrane potential (see example of Na<sup>+</sup> current in Fig. 2). It occurs rapidly in excitable cells and is very steeply dependent upon depolarisation (Hille 1992). Thus, the rate of activation increases with membrane depolarisation. Activation of Na<sup>+</sup> currents generally occurs at thresholds between  $-40$  and  $-60$  mV via the voltage-dependent opening of the 'm' gate (see Fig. 3). The change in voltage opens the channel and allows for a rapid increase in Na<sup>+</sup> permeability. Activation kinetics can be altered by plant alkaloids such as veratridine, scorpion or sea anemone toxins or by insecticides such as pyrethroids (Catterall 1980). This kinetic property is not

**Table 1** Various types of mammalian voltage-gated Na<sup>+</sup> channels

Tissue location	$\alpha$ -subunit	Channel <sup>a</sup>
Heart (human)	SCN5A	Na <sub>v</sub> 1.5
Heart/Denervated skeletal muscle (rat)	SCN5A	Na <sub>v</sub> 1.5
Heart/Uterine muscle (human)	SCN7A	Na <sub>v</sub> 2.1
Heart/Uterine muscle (mouse)	SCN7A	Na <sub>v</sub> 2.3
CNS (human)	SCN1A	Na <sub>v</sub> 1.1
CNS (human)	SCN2A1	Na <sub>v</sub> 1.2
CNS (human/mouse)	SCN8A	Na <sub>v</sub> 1.6
CNS (rat)	SCN1A1	Na <sub>v</sub> 1.1
CNS (rat)	SCN2A1	Na <sub>v</sub> 1.2
CNS (rat)	SCN3A	Na <sub>v</sub> 1.3
PNS (rat)	SCN8A	Na <sub>v</sub> 1.6
PNS (rat DRG)	SCN10A	Na <sub>v</sub> 1.8
Skeletal muscle (human)	SCN4A	Na <sub>v</sub> 1.4
Skeletal muscle (rat)	SCN4A	Na <sub>v</sub> 1.4

<sup>a</sup>According to the standardised nomenclature proposed for Na<sup>+</sup> channels at The IUPHAR/BPS Guide to PHARMACOLOGY website that builds upon and replaces the original IUPHAR Committee on Receptor Nomenclature and Drug Classification Database (IUPHAR-DB). See <http://www.guidetopharmacology.org/> for details  
DRG dorsal root ganglion

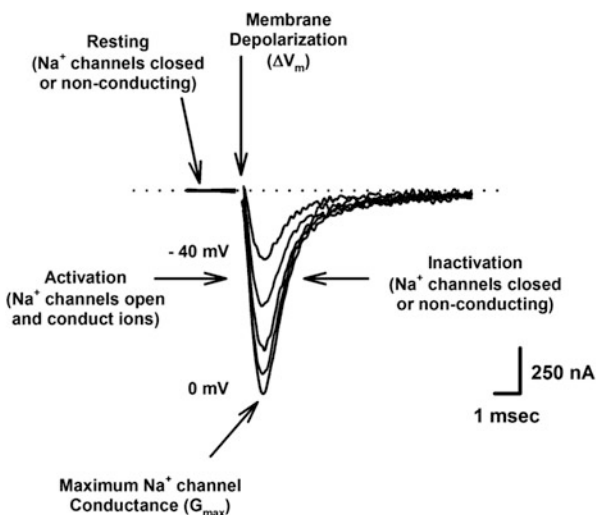


**Fig. 3** A representative family of cardiac Na<sup>+</sup> currents traces evoked in *Xenopus laevis* oocytes. Currents were recorded by two-electrode whole-cell voltage clamp. Oocytes were injected with 50 ng of in vitro transcribed RNA encoding the SkM2 cardiac Na<sup>+</sup> channel  $\alpha$ -subunit. After 2 days of incubation at 20 °C in ND-96 with supplements, currents were evoked by depolarising the cell to -40, -30, -20, -10 and 0 mV from a holding potential ( $V_m$ ) of -120 mV at 3 s intervals. Maximal Na<sup>+</sup> channel conductance ( $G_{max}$ ) was observed when the cell was depolarised to 0 mV. The evoked Na<sup>+</sup> channels all inactivated within  $\approx$ 4 ms after depolarisation

altered by most antiarrhythmic or local anaesthetic drugs such as quinidine or lidocaine. These biological toxins bind to specific binding sites at extracellular sites on the  $\text{Na}^+$  channel and generally shift activation to more negative membrane potentials. Thus, at resting membrane potentials a steady-state depolarisation results that is due to a sustained sodium current. It was originally proposed (for simplicity) that activation was independent of inactivation. However, it was not until Armstrong et al. (1973) perfused the squid giant axon with the enzyme pronase, and showed that inactivation was selectively destroyed and activation was unaltered and that the two processes could be dissociated.

Ionic conductance of the  $\text{Na}^+$  channel is transient in nature. Prolonged depolarisation results in  $\text{Na}^+$  channel inactivation and prevents the influx of  $\text{Na}^+$  into the cell. Thus, refractoriness is maintained. As with activation, the rate of inactivation increases with an increase in the rate of depolarisation (see Fig. 3, panel b). Hodgkin and Huxley (1952) postulated that decay of  $\text{Na}^+$  currents to resting values was mono-exponential. However, Chiu (1977) found that the rate of inactivation was much better approximated with a bi-exponential function and described two voltage-sensitive components for inactivation: fast and slow. Studies by Khodorov et al. (1976) described the slow component and how it was involved in cellular excitability but may have relevance in pathophysiological processes in brain and muscle tissue. Aldrich et al. (1983) used inactivation studies of single channel  $\text{Na}^+$  currents to show that decay was biphasic, and largely coupled to activation, yet slow and fast inactivation are independent events. These studies indicate that some fraction of  $\text{Na}^+$  channels must be open before inactivation proceeds (see Fig. 3). To date, slow inactivation, as a physiological process, remains poorly studied; however, fast inactivation has been extremely well investigated.

The inactivation gate, 'h', can be selectively destroyed by the internal application of protease and chemicals such as the piperazinyl-indole derivative DPI 201-106 (Wang et al. 1990). Veratridine and batrachotoxin, alkaloid toxins, also inhibit inactivation and produce a steady-state depolarisation due to enhanced sodium permeability (Catterall 1980). At the cellular level, this results in a prolongation of the AP and positive inotropism.

Molecular studies have shown that a highly conserved  $\alpha$ -helical intracellular linker between domains III and IV (DIII–DIV) of the sodium channel (see Fig. 2) is responsible for fast inactivation kinetics (Goldin 1993). In addition, these molecular studies provide evidence for the proposed 'ball and chain' model of inactivation whereby this cytoplasmic linker may influence the activation and inactivation coupling process. This model suggests that a positively charged cytoplasmic protein particle (the 'h' gate using Hodgkin and Huxley formalism) electrostatically interacts with a negatively charged inactivation subunit of the sodium channel (Goldin 1993). Three amino acids (IFM) contained within the DIII–DIV loop sequence (isoleucine 1488, phenylalanine 1489 and methionine 1490) are crucial to channel inactivation (West et al. 1992) (Fig. 2). Thus, during inactivation this motif is thought to interact with amino acids that constitute a 'docking' site or

receptor within the pore region and block the pore, impeding the inward movement of  $\text{Na}^+$  ions.

It is important that as a safety pharmacologist that one realises that any NCE in development is not unlike a local anaesthetic or classic antiarrhythmic drug interact with the inactivation gate (Hondegheem and Katzung 1977; Hille 1992). The inactivation produced by a change in membrane potential and drug block of the channel are interacting processes. These occur as a result of drug binding to a site on or near the 'h' gate in a voltage, time and channel state-dependent manner according to the Modulated Receptor Hypothesis (Hille 1992).

Hille in 1977 proposed a model for local anaesthetic action on nerve (Hille 1992). He suggested that there was a single specific binding site for local anaesthetics and that drug occupancy (block) alters the inactivation kinetics of the channel. The proposed location of drug action was intracellular. Hille also postulated that multiple pathways existed for drug access to these binding sites; thus, it could account for all drug access routes to this binding site. Hondegheem and Katzung (1977) used studies in cardiac muscle to propose a similar model for antiarrhythmic drug interaction with cardiac  $\text{Na}^+$  channels. In this cardiac model, a series of equations were developed which defined binding parameters for each state of the channel (rest, open, inactive) and accurately described channel block by quinidine and lidocaine. The general model suggests that as  $\text{Na}^+$  channels change states in a voltage-dependent manner local anaesthetic or antiarrhythmic drugs can associate or dissociate from each state. Thus, each state has a characteristic set of association (k) and dissociation (l) rate constants and voltage and time modulate binding (Hondegheem 1994). Since the affinity for the binding site is modulated by the state of the channel, the proposed model was called the Modulated Receptor Hypothesis (MRH) (Hille 1992; Hondegheem and Katzung 1977).

There is evidence for a specific binding site on the  $\text{Na}^+$  channel for drugs. Ragsdale et al. (1996) identified a putative local anaesthetic, antiarrhythmic and anticonvulsant drug binding site on the S6 transmembrane-spanning region of domain IV (DIVS6) that lines the pore of the  $\text{Na}^+$  channel (see Fig. 2). Additional delineation of the amino acids involved in drug binding suggests that pore-lining residues in the S6 region of domain III (DIIS6) may also be involved in drug binding.

The existence of a persistent or 'late'  $\text{Na}^+$  channel has been proposed for decades (Saint 2007). While the physiological role for the late  $\text{Na}^+$  channel remains unknown, it has similar biophysical properties to the fast (or transient)  $\text{Na}^+$  channel including ion channel selectivity and single channel conductance properties, but the population of ion channels that constitute the late channels fail to inactivate after opening (Saint 2007). The late  $\text{Na}^+$  current is pharmacologically distinct and appears more sensitive to block by tetrodotoxin (TTX) and lidocaine as well as ranolazine and vernakalant (Ju et al. 1992; Saint et al. 1992). While the magnitude of the late  $\text{Na}^+$  current in the normal heart is small (~1 % that of the fast  $\text{Na}^+$  current), its magnitude is increased in many pathologic conditions including ischaemia (see Zaza et al. 2008). An enhanced cardiac late  $\text{Na}^+$  current is proarrhythmic (i.e. elicits EADs, triggered arrhythmic activity, and TdP) an effect



that has been demonstrated in many SP assays including isolated Purkinje fibres, coronary-perfused wedge preparations and Langendorff hearts (Saint 2007; Zaza et al. 2008). This cardiac  $\text{Na}^+$  current is currently being considered as a component to the CIPA ion channel assay.

With an understanding of the cardiac  $\text{Na}^+$  channel complete, a return of the membrane potential to its pre-depolarising (resting) level begins with activation of  $\text{Ca}^{2+}$  current and repolarising  $\text{K}^+$  currents.

---

## 6 Cardiac Calcium Channels

Voltage-gated  $\text{Ca}^{2+}$  channels are important regulators of electrical signalling and mechanical function in the heart. Calcium is an important ion to the myocyte (and to all cells) as it acts as an intracellular messenger in the initiation and/or regulation of many cellular processes including gene expression, enzyme function and cardiac muscle contraction.

At the myocyte level,  $\text{Ca}^{2+}$  is highly regulated both at the cell membrane and at intracellular loci (organelles) where concentrations  $\approx 10^{-8}$  M are maintained. At the cell membrane, regulation is mediated by voltage-gated  $\text{Ca}^{2+}$  channels, by  $\text{Ca}^{2+}$  pumps and by the  $\text{Na}^+/\text{Ca}^{2+}$  exchanger. At intracellular loci, the sarcoplasmic reticulum, endoplasmic reticulum and mitochondria regulate  $\text{Ca}^{2+}$  levels. With such a complex hierarchical distribution and functional display by the  $\text{Ca}^{2+}$  ion, a number of voltage-gated channels exist that gate only this ion in excitable cells.

### 6.1 Molecular and Pharmacological Properties

Calcium channels are responsible for the genesis of APs in cardiac pacemaker cells (diastolic depolarisation) and the propagation of slow APs in sino-atrial and atrio-ventricular node cells and are equally important in the control of depolarisation-induced  $\text{Ca}^{2+}$  entry responsible for the plateau (phase 2) of the AP (see Fig. 1).

Voltage-gated  $\text{Ca}^{2+}$  channels are hetero-oligomeric protein complexes that are comprised of an  $\alpha_1$ - ( $\approx 240$  kDa) subunit, a  $\beta$ -subunit ( $\approx 60$  kDa) and an accessory  $\alpha_2 - \delta$  ( $\approx 175$  kDa) subunit (Striessnig 1999). At least six classes of voltage-gated  $\text{Ca}^{2+}$  channel have been characterised. Cloning studies reveal that these channels exist in various tissues as a result of the co-assembly into protein complexes with variable accessory subunits (see Table 2). Expression in heterologous systems has allowed for their electrophysiological and pharmacological characterisation. There is a single L-type and five non-L-type channels called T, N, P/Q and R (Ertel et al. 2000). These channels can be further subdivided into those that exhibit low voltage-activating (LVA) properties and rapidly inactivate (properties of the T-type channel isoform) and those that are highly voltage-activated (HVA) and do not inactivate.

Each of the  $\alpha_1$ -subunits of the  $\text{Ca}^{2+}$  channel, composed of approximately 1,800 amino acid residues, is the major protein constituent that contains the ionic pore, the

**Table 2** Types of mammalian voltage-gated calcium channels

Tissue location	$\alpha$ -subunit	Gene	Channel
Heart (rat)	$\alpha_{1C}$	CACNA1C	L-type
Heart (rat)	$\alpha_{1G}$	CACNA1G	T-type
Heart (human)	$\alpha_{1H}$	CACNA1H	T-type
CNS/NMJ	$\alpha_{1A}$	CACNA1A	P/Q-type
CNS/NMJ	$\alpha_{1B}$	CACNA1B	N-type
CNS/NMJ	$\alpha_{1E}$	CACNA1E	R-type
Retina	$\alpha_{1F}$	CACNA1F	L-type
Skeletal muscle	$\alpha_{1S}$	CACNA1S	DHP

*Note:* L- and T-type channels are found in cardiac muscle where they are sensitive to blockade by pharmacological agents including verapamil and diltiazem

selectivity filter, intracellular regulatory regions and necessary gating machinery of the channel (see Fig. 4). Ten  $\alpha_1$ -subunit genes have been identified as  $\alpha_{1A} - \alpha_{1I}$  and  $\alpha_{1S}$ . In cardiac ventricular muscle, only the  $\alpha_{1C}$ -subunit encoding the L-type  $\text{Ca}^{2+}$  channel is found at appreciably high levels (>80 %) while  $\alpha_{1D}$ -subunit expression is found in atrial muscle (Striessnig 1999; Ertel et al. 2000). Of the three isoforms of the  $\alpha_1$ -subunit that encode for the T-type channels (see Table 2), only  $\alpha_{1G}$  and  $\alpha_{1H}$  are found in cardiac tissue.

The  $\alpha_1$ -subunit also contains the binding domain for  $\text{Ca}^{2+}$  channel antagonist drugs. The L-type channel, which carries  $I_{si}$  in the heart, is blocked by three groups of drugs. The phenylalkylamine (e.g. verapamil) and benzothiazepine (e.g. diltiazem) blockers are effective clinically used antiarrhythmics while the 1,4-dihydropyridines (e.g. nifedipine) are useful antihypertensive agents. Chemically,  $\text{Ca}^{2+}$  channels show a marked structural homology to each other and to voltage-gated  $\text{Na}^+$  channels. This subunit is composed of four homologous domains (DI–DIV), each of which is composed of six transmembrane-spanning  $\alpha$ -helical proteins that form a pore in the membrane (see Fig. 4). Like  $\text{Na}^+$  channels, the fourth transmembrane helix (S4) contains positively charged amino acids which are responsible for the gating or voltage-sensing activity of the channel. The sixth transmembrane helix of each domain is responsible for conferring inactivation properties to the channel.

Calcium channels, like many other voltage-gated ion channels, require auxiliary subunits for functional expression. Currently four mammalian isoforms of the  $\beta$ -subunit exist. These polypeptides vary between 52 and 71 kDa and are involved in membrane stabilisation and trafficking of the  $\alpha_1$ -subunit within the cell (DeWaard et al. 1994). Note that the cardiac L- and T-type  $\text{Ca}^{2+}$  channels are only co-expressed with the  $\beta_2$ -subunit isoform. Of the three  $\alpha_2 - \delta$  subunit isoforms that have been detected in various tissues, only the  $\alpha_2 - \delta_1$  and  $\alpha_2 - \delta_2$  types are expressed in the heart (Klugbauer et al. 1999). The  $\alpha_2$  component is a highly glycosylated extracellular protein that associates with extracellular regions of the  $\alpha_1$ -subunit and stabilises drug binding while the  $\delta$  component may stabilise channel gating properties (Striessnig 1999).

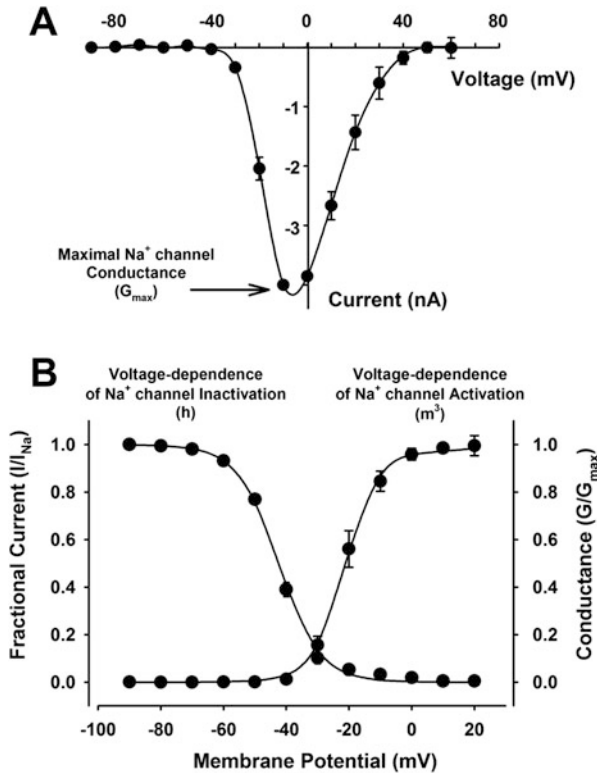


**Fig. 4** Biophysical properties of cardiac voltage-gated  $\text{Na}^+$  ion channels. Panel (a) depicts the current–voltage relationship for the cardiac rH1  $\text{Na}^+$  current isoform expressed in *Xenopus* oocytes. Cells were held at a membrane potential of  $-120$  mV and currents were measured by depolarisations ranging from  $-90$  to  $+50$  mV in  $10$  mV increments. Sodium channel conductance ( $G_{\text{max}}$ ) was maximal at a depolarising potential to  $-10$  mV. The data are plotted as peak current amplitude versus the pulse potential and the curve for the figure is the best fit of the equation:  $I = G_{\text{max}}/1 + \exp[(V - V^*)/k] (V - E_{\text{rev}})$  (see text for details). Panel (b) shows the voltage dependence of  $\text{Na}^+$  channel activation ( $\text{m}^3$ ) and inactivation (h) for the cardiac rH1 isoform expressed in oocytes. The voltage dependence of  $\text{Na}^+$  channel activation or conductance ( $G/G_{\text{max}}$ ) was calculated by measuring the peak current at test potentials ranging from  $-90$  mV to  $+20$  mV evoked in  $10$  mV increments and dividing by  $(V - V_{\text{rev}})$ , where  $V$  is the test potential and  $V_{\text{rev}}$  is the reversal potential for  $\text{Na}^+$ . Peak conductance values were fit with a two-state Boltzmann equation of the form  $G = 1/[1 + \exp(-0.03937 \cdot z_{\text{app}} \cdot (V - V_{1/2})]$ . The voltage dependence of steady-state inactivation was determined using  $500$  ms conditioning pre-pulses from a holding potential of  $-120$  mV to  $+15$  mV in  $10$  mV increments, followed by a test pulse to  $-5$  mV for  $22.5$  ms. The peak current amplitude evoked during the test depolarisation was normalised to the maximum current amplitude and plotted as a function of the conditioning pre-pulse potential. The data were fit with a two-state Boltzmann equation of the form  $I = I_{\text{max}}/[1 + (\exp(V - V_{1/2})/k)]^{-1}$

As mentioned above, the  $\alpha_1$  isoforms determine the pharmacological properties of each of the  $\text{Ca}^{2+}$  channels in the heart. The L-type  $\text{Ca}^{2+}$  channels possess high-affinity, stereoselective-binding domains for channel blocking drugs, and thus blockade of these  $\text{Ca}^{2+}$  channels in the heart exerts antiarrhythmic activity against

supraventricular arrhythmias. A combination of complementary photo-affinity labelling, antibody mapping and cloning studies of the various  $\alpha_1$ -subunits present in the heart suggests that it is the S6 regions of domains III and IV and the S5–S6 linker of domain III that may contain the actual high-affinity binding sites for channel blocking drugs. All  $\text{Ca}^{2+}$  channel blocking drugs bind with close proximity to the pore and as a result of their binding alter the actual binding site for  $\text{Ca}^{2+}$  ions within the pore (Fig. 4). These actions have been used to explain the non-competitive allosterism that is observed for various blocking drugs on many  $\text{Ca}^{2+}$  channel preparations. The binding of channel blocking drugs is suggested to produce conformational changes in amino acids in this region, which then alter pore-associated binding properties to  $\text{Ca}^{2+}$  ions.

Unlike the L-type cardiac  $\text{Ca}^{2+}$  current, the T-current rapidly inactivates and is involved in pacemaker activity in the sino-atrial node and intracellular  $\text{Ca}^{2+}$ -induced  $\text{Ca}^{2+}$  release.

---

## 7 Cardiac Potassium Channels

### 7.1 Diversity of Voltage-Gated Potassium Channels

During the 1980s and into the 1990s, interest in the development of drugs which prolong refractoriness, i.e. possess class III antiarrhythmic action, had increased markedly. Several reasons for this resurgence in interest included the negative results of the CAST trials where proarrhythmic tendencies were associated with some class I agents and the effectiveness of long-term studies with amiodarone which suggested that it may, in a manner similar to the  $\beta$ -blockers, decrease post-infarction arrhythmic death (Vaughan Williams 1984). Repolarisation and the configuration of phase 3 of the AP in cardiac tissue occur as a result of the complex interaction of multiple  $\text{K}^+$  channels (Snyders 1999). These  $\text{K}^+$  channels are heterogeneous and differ in gating and permeation properties as well as in susceptibility to modulation by neurotransmitters, intracellular ions such as  $\text{Na}^+$  and  $\text{Ca}^{2+}$  and NCEs. In essence,  $\text{K}^+$  channels regulate cell function by establishing the resting membrane potential and controlling cell repolarisation processes. Individual  $\text{K}^+$  currents overlap in their contribution to the total membrane current during the AP. The relative importance of each may vary under different conditions; for example, during ischaemia changes in cell electrophysiology may alter the degree to which different channels contribute to the AP.

Amongst ion selective channels within the myocardium, the  $\text{K}^+$  channel is unrivalled in terms of molecular and functional diversity. As the genetic, molecular and functional diversity of  $\text{K}^+$  channels grows so does the general complexity with regard to its pharmacology and nomenclature. In general, mammalian  $\text{K}^+$  channels have been categorised into three main families: the voltage-gated  $\text{K}^+$  channels ( $K_v$ ), the inward rectifying  $\text{K}^+$  channels ( $K_1$ ) and the two pore domain channels ( $K_{2P}$ ) (see Table 3). However, the literature is rife with creative modifications to this simple classification scheme. For the purposes of the present discussion, channels will be

**Table 3** Types of mammalian cardiac voltage- and ligand-gated potassium channels

Cardiac current	$\alpha$ -Subunit clone
Transient outward ( $I_{to}$ )	
Fast component ( $I_{to,f}$ )	$K_v4.2/K_v4.3$
Slow component ( $I_{to,s}$ )	$K_v1.4$
Delayed rectifier ( $I_K$ )	
Rapid component ( $I_{Kr}$ )	$K_v11.1$ (hERG)
Slow component ( $I_{Ks}$ )	$K_vLQT1 + \text{min K}$
Ultra-rapid component ( $I_{Kur}$ )	$K_v1.5$
Inward rectifier ( $I_{K1}$ )	
$I_{K1}$	Kir2.1
( $I_{KATP}$ )	Kir6.2 + SUR2A
( $I_{KAch}$ )	(GIRK) Kir3.4 + Kir3.1
Pacemaker current ( $I_f$ )	HCN4

described using the classification system mentioned above, but safety pharmacologists should be aware of alternate names for these channels. Refer to the IUPHAR/BPS Guide to PHARMACOLOGY website for the latest detailed list of ion channel nomenclature (Pawson et al. 2014).

Genes that encode the nucleotide sequence(s) responsible for the expression of functional  $K^+$ -selective ion channels in the myocardium are distributed widely throughout the genomes of many diverse species. These include yeast (*S. lividans* and *S. cerevisiae*), the nematode *C. elegans*, the fruit fly (*D. melanogaster*), the cyanobacteriae (*A. thaliana*), the mouse (*M. musculus*) and humans (*H. sapiens*). In some instances, the gene sequences and functional characteristics of the channels themselves are highly conserved across species (MacKinnon et al. 1998). Note that mutations in  $K^+$  channel genes may be responsible for certain types of cardiac pathology that may or may not be dependent upon environmental factors (e.g. idiopathic long QT syndrome and hypokalemia) (Roberts and Brugada 2000).

In general, all  $K^+$  currents have a similar primary amino acid sequence with highly conserved structural regions (see Fig. 5). The molecular structures of  $K^+$  channels may be described as having one or two pore-forming domains and two, four or six transmembrane-spanning domains (collectively referred to as the  $\alpha$ -subunit). The molecular diversity of  $K^+$  channels, like the  $Ca^{2+}$  channels described above, is largely due to variability in the heteromeric association of pore-forming  $\alpha$ -subunits and accessory, or  $\beta$ -subunits, during formation of channel complexes (Nerbonne 2000). Voltage- and  $Ca^{2+}$ -dependent  $K^+$  channel  $\alpha$ -subunits exhibit six transmembrane-spanning sequences with a voltage sensor in S4 and a pore-forming region located between S5 and S6 (see Fig. 6). Inwardly rectifying  $K^+$  channel  $\alpha$ -subunits are comprised of two transmembrane-spanning sequences and like the voltage-gated channels have one pore-forming region. Other  $K^+$  channels that exhibit little or no voltage-dependent action but are modulated by pH, stretch, temperature and a variety of second messengers are formed through the dimerisation (sometimes requiring a cysteine residue) of  $\alpha$ -subunits containing two pore-forming sequences and four transmembrane sequences. The common

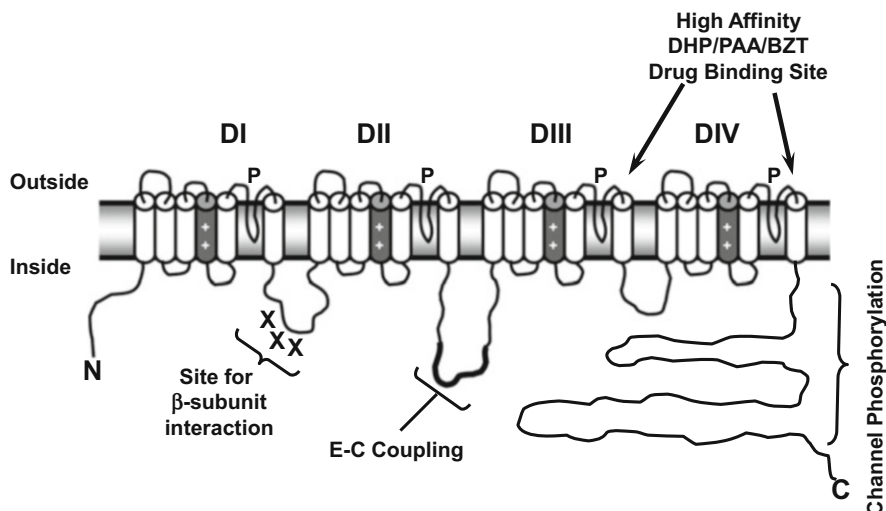


**Fig. 5** A schematic of the proposed molecular structure of the  $\text{Ca}^{2+}$  channel present in the heart. This model depicts the transmembrane folding of the primary structure of the  $\text{Ca}^{2+}$  channel  $\alpha$ -subunit. The domains of the channel are indicated as DI–DIV. The six  $\alpha$ -helical transmembrane-spanning sequences are shown for each domain. Transmembrane segment S4, the channel voltage sensor, is depicted with (+) residues and those regions associated with formation of the channel pore as P. Some experimentally determined sites for  $\beta$ -subunit interaction, channel phosphorylation and excitation–contraction (EC) coupling are shown along with the putative  $\alpha$ -helices important for the high affinity of dihydropyridine (DHP), phenylalkylamine (PAA) and benzothiazepine (BTZ) drugs

feature amongst these different channel-forming strategies is that the ion selective pore is always formed by the fusion of four pore-forming segments. Also,  $\text{K}^+$  channels all commonly contain regulatory sites on both amide and carboxyl terminal sequences. Similar sites are also located on the  $\beta$ -subunits that in turn directly modify  $\alpha$ -subunit function (Nerbonne 2000).

The functional properties of currents carried by  $\text{K}^+$  channels range from those with strong time- and voltage-dependent activation and inactivation kinetics with an associated strong inward or outward rectification (e.g. as seen with  $I_{\text{Kr}}$ ) to time- and voltage-independent activation and inactivation kinetics with very weak rectification (e.g. as seen with  $I_{\text{TWIK-1}}$ ). Voltage-dependent activation of  $\text{K}^+$  currents plays a considerable role in the repolarisation of the cardiac cell membrane whereas constitutive activation of  $\text{K}^+$  currents that are voltage *independent* may play roles in both repolarisation and maintenance of the cell resting membrane potential. Voltage-dependent inactivation may proceed either rapidly or slowly by N- and C-type inactivation, respectively (Rasmusson et al. 1998). Cardiac  $\text{K}^+$  channels that activate and inactivate rapidly (such as the fast component of the transient outward  $\text{K}^+$  current,  $I_{\text{to,f}}$ ), slowly (such as the slow component of the delayed rectifier  $\text{K}^+$  current,  $I_{\text{Ks}}$ ) or at variable rates (such as the ultra-rapid component of the delayed

## Molecular Correlates of Voltage-Gated K<sup>+</sup> Channels

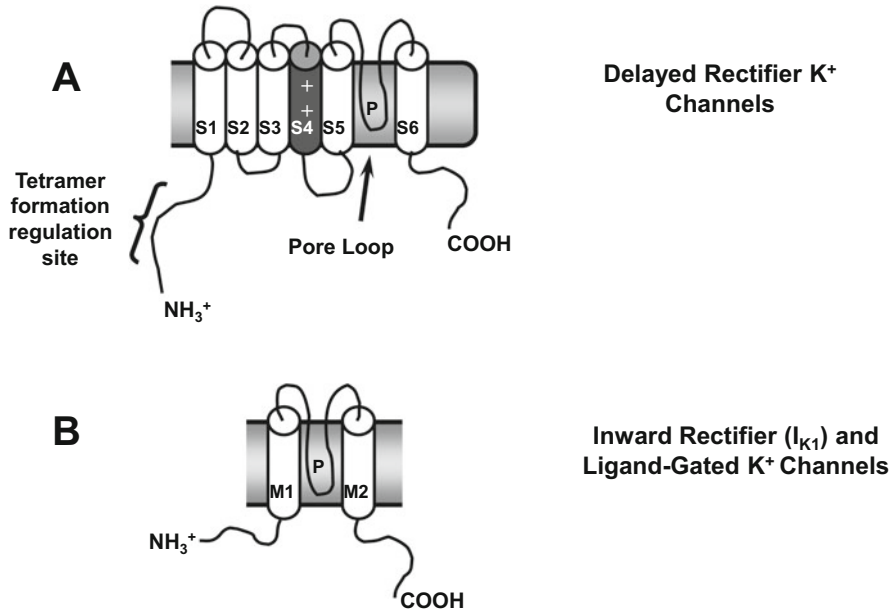


**Fig. 6** Molecular correlates of some native voltage- and ligand-gated K<sup>+</sup> channels found in cardiac muscle. Panel (a) depicts the putative molecular model shared by delayed rectifier (*I<sub>K</sub>*) and transient outward (*I<sub>to</sub>*) K<sup>+</sup> channels. These subunits contain six transmembrane segments (S1–S6) and one P-loop for the mammalian channel clones *K<sub>v</sub>1.x – K<sub>v</sub>4.x* (*I<sub>K</sub>* and *I<sub>to</sub>*), *HERG* (*I<sub>Kr</sub>*) or *K<sub>v</sub>LQT1 + minK* (*I<sub>Ks</sub>*). Panel (b) depicts subunits that encode the inward rectifier (*I<sub>K1</sub>*) and several ligand-gated K<sup>+</sup> currents including *I<sub>KATP</sub>* and *I<sub>KAch</sub>*. These channels contain only two transmembrane segments (M1 and M2) and one P-loop for the mammalian channel clones *Kir2.1* (*I<sub>K1</sub>*), *Kir6.2 + SUR1* (*I<sub>KATP</sub>*) and *Kir3.1 + Kir3.4* (*I<sub>KAch</sub>*)

rectifier K<sup>+</sup> current, *I<sub>Kur</sub>*) will therefore contribute differently to cardiac cell excitability and repolarisation under different circumstances (e.g. at fast or slow heart rates). Potassium channels may have very diverse mean open times such that some channels may be open as briefly as 1 ms or remain open for hundreds of milliseconds. Single channel conductance through the open cardiac K<sup>+</sup> channel may be low in some channels (such as <5 pS in the two-pore domain K<sup>+</sup> channel *I<sub>TWIK-2</sub>*), moderate in others (such as 20–30 pS in the transient outward K<sup>+</sup> channel, *I<sub>to</sub>*) and high in others (such as >100 pS in the TWIK-related K<sup>+</sup> channel *I<sub>TREK-1</sub>*). Note however that ion channel conductance depends upon the expression system employed (i.e. is the system native or heterologous or involve stem cell differentiation and expression?) and the recording environment (i.e. currents should be recorded using the whole-cell configuration of the patch clamp and utilise physiologically relevant K<sup>+</sup> concentrations used to delineate channel activity). Such criteria should be strictly defined in any SP electrophysiology study and strive

for physiological relevance in order to optimise biophysical properties of  $K^+$  channels in cardiac tissue to best characterise any potential for interactions with NCEs.

Currents carried by  $K^+$  channels are therefore extremely important in the regulation of myocardial cell resting potential and repolarisation and, thus, to the configuration of the cardiac AP and ECG morphology. The differential distribution of  $K^+$  channels within the myocardium accounts for the large variation in  $K^+$  current density, AP morphology within different cells of the heart and in AP and ECG morphology across species (Yan and Antzelevitch 1996; Yan et al. 1998). The abundance of  $K^+$  channel mRNA can vary dramatically in different cell types (see below for more detail). The combined effects of highly varied  $K^+$  channel type and subtype expression, function and regulation converge in the myocardium to produce a complex effect on the electrical excitability of cardiac cells and the morphology of recorded electrical activity in normal, diseased and drug-treated hearts.

Traditionally  $K^+$  channels have been characterised pharmacologically based on their sensitivity to tetraethylammonium (TEA), 4-aminopyridine (4-AP) or cations such as cesium ( $Cs^+$ ) and barium ( $Ba^{2+}$ ). More recently, naturally occurring venoms such as that isolated from the scorpion and synthetic compounds including dofetilide, astemizole, E-4031, JNJ-202 and Chromanol 293B have been used to successfully isolate and study specific components of different  $K^+$  channel currents. While  $K_v$  channels are ubiquitously sensitive to blockade by either TEA or 4-AP, they exhibit a differential sensitivity to a range of cardiovascular and non-cardiovascular drugs in normal (and diseased) myocardium (Yang and Roden 1996).

The inward rectifying  $K^+$  channels ( $K_{ir}$ ) couple direction of  $K^+$  flow in the myocyte (inward *against* the normal  $K^+$  ion concentration gradient) to the metabolic status of the myocardium. These channels are commonly activated or blocked by the products of cellular metabolism and by various cations. The  $K_{IR}$  family is composed of a large number of channel subtypes; some are voltage dependent while others are not. In addition, some channels in this group are ATP sensitive ( $I_{KATP}$ ) or GTP activated. Many synthetic and naturally occurring drugs can activate (benzopyrans) or block (sulfonylureas)  $I_{KATP}$  currents in cardiac and non-cardiac (pancreatic) tissue providing these channels as good clinical targets for drug development.

The safety pharmacologist should be aware of the differences that single or multiple nucleotide polymorphisms (SNP) make in the gene sequences of various  $K^+$  channels that result in the expression of ion channel proteins with either severe or subtle changes in biophysical properties. While these proteins may perform most functional tasks sufficiently such that myocyte function is not significantly impeded, drug properties may change and hence unanticipated clinical adverse events such as prolongation of the QT interval could occur or precipitate other untoward adverse responses of the myocyte to drugs in the clinical population. Therefore changes in  $K^+$  channel structure can contribute to a number of congenital or drug-induced cardiac disorders including the long QT syndrome, idiopathic



polymorphic VT, Andersen's Syndrome and the Jervell and Lange-Nielsen Syndrome.

Thus, the heterogeneity of  $K^+$  channels provides for a large potential for NCEs in development to potentially block  $K^+$  channels. This is well documented within the drug safety literature where the therapeutic potential and benefits of these agents were dashed by their ability to precipitate TdP arrhythmias (Pugsley 2002).

An important property that should be understood when assessing the safety profile with regard to blockade of K channels is that prolongation of the APD occurs optimally at low rates of stimulation while are limited at high heart rates. This 'reverse use dependence' is an important drug property to characterise with any drug as it suggests that mechanistically these drugs may have a high affinity for the closed state of the  $K^+$  channel (Pugsley 2002). Only amiodarone lacks this effect. The resulting bradycardia associated with potent and selective  $I_{Kr}$  channel blockade is known to precipitate arrhythmias such as the prolonged Q-T and TdP.

Of the many  $K^+$  channels that exist in cardiac muscle, we will provide an overview of only those  $K^+$  conductances which carry most of the outward repolarising current and that are important in understanding the basis for development of the CIPA paradigm for SP. These include only the transient outward ( $I_{to}$ )  $K^+$  current, the delayed rectifier  $K^+$  ( $I_K$ ) current and its components that contribute predominantly during the plateau and early stages of repolarisation of the AP and the inward rectifier ( $I_{KIR}$ )  $K^+$  channels.

## 7.2 Voltage-Dependent ( $K_V$ ) Transient Outward ( $I_{to}$ ) and Delayed Rectifier ( $I_K$ ) Channels

The voltage-dependent  $K^+$  currents ( $K_V$ ) that have the greatest influence on changes in cardiac cellular resting membrane potential, especially repolarisation, are the transient outward ( $I_{to}$ ) and the delayed rectifier ( $I_K$ )  $K^+$  currents and their many subtypes (Nerbonne 2000).  $K_V$  channel  $\alpha$ -subunits are derived from six families of channel proteins, most of which are based on the *D. melanogaster* nomenclature (*Shaker*, *Shab*, *Shaw*, *Shal*, *Eag* and  $K_V$ LQT1). The genes responsible for the mammalian cardiac  $\alpha$ -subunits that produce the pore-forming regions and some of the  $\beta$ -subunits that modify channel expression and function are distributed widely throughout the genome. In most cases, the  $K_V$  genes are transcribed according to the same mechanisms that operate for transcription of other voltage-dependent ion channels. Large conductance  $Ca^{2+}$ - and voltage-activated  $K^+$  channels are also found within the myocardium; however, these ion channels are predominantly expressed in neurons and vascular smooth muscle cells and will therefore not be discussed here.

### 7.2.1 Molecular Genetics of $I_{to}$ and $I_K$ Channels

All  $K_V$  channels are comprised of four  $\alpha$ -subunits and may co-assemble with at least one of four possible  $\beta$ -subunits.  $K_V$   $\alpha$ - and  $\beta$ -subunits co-assemble within the endoplasmic reticulum and exhibit chaperone-dependent trafficking to the

membrane surface (Kuryshv et al. 2001). Each  $\alpha$ -subunit (see Fig. 5 for details) consists of six transmembrane-spanning sequences (S1–S6) that perform a variety of functions including voltage sensing (the S4 region), rapid N-type inactivation (the N-terminal and S5 region), slower C-type inactivation (the H5 pore loop and S6 region) and intracellular communication (the C-terminal) (Armstrong and Hille 1998).  $K_V$  channels are unique compared to their inward rectifying counterparts in that functional channels may form through the heteromeric association of  $\alpha$ -subunits and that subunit dosage may regulate membrane trafficking of functional channels. The molecular correlates of heteromeric  $\alpha$ -subunit channels have been the subject of intense investigation in a number of tissues and in a variety of species (Nerbonne 2000).

The transient outward  $K^+$  channel ( $I_{to}$ ) is a relatively common current found in a wide variety of species and cell types. The channel possesses rapid activation and inactivation kinetics and is important during early phase I repolarisation (Coraboeuf and Carmeleit 1982). It is coupled to both  $Na^+$  and  $Ca^{2+}$  and is critical for the classic ‘spike and dome’ appearance of the ventricular AP. Channel density and distribution differences amongst cell type’s results in a variable AP morphology in various regions of the heart.  $I_{to}$  are composed of a large voltage-activated,  $Ca^{2+}$ -independent component,  $I_{to,f}$  (or  $I_{to1}$ ), and a small  $Ca^{2+}$ -activated component,  $I_{to,s}$  (or  $I_{to2}$ ), and the channel activates at membrane potentials more positive than  $-70$  mV and inactivates at  $-10$  mV (Coraboeuf and Carmeleit 1982).  $I_{to}$  is highly  $K^+$  selective, shows little rectification, reaches its peak in 3 ms and, depending on the species, shows either mono- or bi-exponential rates of inactivation (Jahnel et al. 1994). In the rat,  $I_{to}$  is the main repolarising current and is sensitive to blockade by 4-aminopyridine (4-AP) and tedisamil (Beatch et al. 1991).

The fast component of the transient outward current ( $I_{to,f}$ ) is comprised of predominantly  $K_V4.2$  and  $K_V4.3$   $\alpha$ -subunits; however, it depends upon the selection of cardiac tissue whereas the slow component ( $I_{to,s}$ ) is primarily composed of  $K_V1.4$   $\alpha$ -subunits (Wickenden et al. 1999). Modulation of both  $I_{to}$  and  $I_K$  currents by accessory  $\beta$ -subunit proteins is important, especially in many cardiac pathophysiological diseases.

The time- and voltage-dependent  $K^+$  current ( $I_K$ ) channel, also called the ‘delayed rectifier’, is governed by a single voltage-dependent gate that activates slowly. The  $G_{max}$  for this channel shows some slight ‘inward rectification’, i.e. the current decreases markedly with depolarisation. This rectification is in the opposite direction to that predicted by the GHK current equation. This current is dependent upon extracellular  $K^+$  and because the channel has appreciable  $Na^+$  permeability  $V_K$  is less negative than the Nernst potential for  $K^+$ . The slowness of activation of the  $I_K$  channel may be regarded as permitting the prolonged plateau of the cardiac AP (phase 2), despite slow inactivation of voltage-dependent  $Ca^{2+}$  channels and its eventual activation as principally responsible for terminating phase 2. The sensitivity of  $I_K$  to extracellular  $K^+$  accounts very largely for the phenomenon whereby phase 2 is prolonged (and repolarisation, phase 3, delayed) when extracellular  $K^+$  is lowered, and the reverse when it is raised. The delayed rectifier  $K^+$  current ( $I_K$ ) has (at least) two components, one relatively large and slow to activate ( $I_{Ks}$ ) and the

other small and more rapidly activating ( $I_{Kr}$ ). Currently a number of  $I_K$  channel types have been cloned and are comprised of many channel subtypes that result from the functional assembly of  $K_V1.1$ ,  $K_V1.2$ ,  $K_V1.5$ ,  $K_V2.1$ ,  $K_V2.2$ ,  $K_V3.1$ ,  $K_VLQT1$  and HERG  $\alpha$ -subunits (Nerbonne 2000).

### 7.2.2 Functional and Pharmacological Properties

The functional properties of most  $K_V$  channels have been described in detail in native and heterologous expression systems and the effects of modifications to various regions of the S1–S6 transmembrane sequences of the  $\alpha$ -subunits have been well characterised (Boyett et al. 1996). Both of the  $I_{to}$  channel subtypes activate early and the distinguishing functional feature that arises between  $I_{to,f}$  and  $I_{to,s}$  current involves their rates of channel inactivation and recovery from inactivation. While  $I_K$  currents activate at variable rates, they all tend to inactivate slowly, or very slowly, with the inactivation kinetics of  $I_{Kr}$  being the only exception and a unique identifier of that current. Native and heterologously expressed  $K_V4.2$  and  $K_V4.3$  channels exhibit sensitivity to protein kinase C (PKC) that is manifest as a reduction in outward  $K^+$  current due to changes in inactivation kinetics and recovery from inactivation (Nakamura et al. 1997). The voltage-dependent, ultra-rapidly activating  $K^+$  current ( $I_{Kur}$ ) is sensitive to protein kinase A (PKA)-mediated phosphorylation and it is known that the PKA regulation of  $K_V1.5$  channel function is mediated by a specific set of N-terminal residues on the  $K_V\beta1.3$  subunit (Kwak et al. 1999). In native atrial myocytes  $\alpha$ - and  $\beta$ -receptor mediated adrenergic stimulation may significantly modify members of the  $I_K$  family such as  $I_{Kur}$  via interactions with PKC and PKA (Yue et al. 1999). Therefore,  $K_V$  channels are not only unique with regard to their regulation by voltage but also exhibit sensitivity to modification by the intracellular and extracellular myocardial environment, a sensitivity that may enhance the potential for pharmacological regulation of  $K_V$  channels.

Like the functional properties of  $K_V$  channels, the pharmacology of native and cloned  $K_V$  channels has been described in considerable detail (Rolf et al. 2000). However, one should note that there are key aspects of  $K_V$  channel pharmacology which produce significantly different effects under either normal or pathological cardiac conditions. It remains very difficult to isolate specific channel subtypes in vitro due to (1) contamination of preparations by other  $K^+$  currents, (2) poor selectivity of subtype-specific blocking agents and (3) the inability to measure gross electrophysiological variables (APD, ERP) using cloned channels in heterologous expression systems. The reverse use dependence associated with drugs interacting with  $K^+$  channel has been rigorously investigated. Reverse use dependence is a pronounced pharmacological phenomenon associated with  $K_V$  channel block and should be an electrophysiological parameter of assessment in drug safety studies.

Pharmacologically,  $I_{to,f}$  and  $I_{to,s}$  can be distinguished by their sensitivity and insensitivity, respectively, from the class Ic antiarrhythmic drug, flecainide and the heteropodatoxins (Xu et al. 1999). The pharmacology of  $K_V$  channels is complex. Several examples of the complexity are given. The rapid ( $I_{Kr}$ ) and slow ( $I_{Ks}$ ) activating components of  $I_K$  are readily distinguishable based upon their sensitivity and insensitivity, respectively, to methanesulfonamide drugs such as dofetilide and

E-4031 and the cation  $\text{La}^{3+}$  (Main et al. 1998).  $I_{K_{\text{ur}}}$  or the  $K_{\text{v}}1.5$  channel is present in human atrial tissue. It is outwardly rectifying and highly selective for  $\text{K}^+$ . Like other  $K_{\text{v}}$  channels it activates during the plateau phase of the cardiac AP and is distinguished from related  $K_{\text{v}}$  channels by its sensitivity to very low concentrations of extracellular 4-AP.  $I_{K_{\text{s,slow}}}$  is another distinct  $K_{\text{v}}$  channel represented by  $K_{\text{v}}1.2$  expression (Nerbonne 2000). It is sensitive to block by very low concentrations of 4-AP but unlike  $I_{K_{\text{ur}}}$  this current is sensitive to nanomolar concentrations of dendrotoxin (DTX) and thus may be designated as  $I_{K_{\text{,DTX}}}$  (Nerbonne 2000).

As a result of its rapid voltage-sensitive activation and inactivation,  $I_{\text{to,f}}$  contributes substantially to the very early phase of repolarisation prior to the AP plateau. It exhibits marked, variable expression patterns in cardiac tissue. These differences in gradients for the expression of  $K_{\text{v}}4.2$  proteins exist at all levels in the heart including transmurally where  $I_{\text{to,f}}$  is present at high levels in the epicardium and at low levels in the endocardium, interventricularly where it is present at greater levels in the right compared to the left ventricle, intraventricularly where  $I_{\text{to,f}}$  is present in the apex and septum, but  $I_{\text{to,s}}$  is present in the septum only, and longitudinally where  $I_{\text{to,f}}$  is greater in the apex than the base of the heart. These differences therefore account for the sharp spike and dome appearance of APs obtained from the epicardium compared to the endocardium as well as for differences in the spike and dome morphology in epicardial cells from different species and may account for the varied J–T interval duration and S–T segment elevation observed between species. For example, ventricular  $K_{\text{v}}4.2$  subunit levels are greatest in the rat and non-existent in the guinea pig (rat > dog > human >>> guinea pig) (Nakamura et al. 1997; Gussak et al. 2000). Interestingly, small and large mammals may regulate the expression profiles of functional  $K_{\text{v}}4$  channels via different mechanisms.

Like  $K_{\text{v}}4$  channels,  $\text{K}^+$  channels that carry the many varieties of  $I_{\text{K}}$  currents also exhibit differential expression profiles within the mammalian myocardium. In dogs and humans,  $I_{\text{K}_{\text{r}}}$  densities are larger in left versus right atrium whereas  $I_{\text{K}_{\text{s}}}$  current densities exhibit an even distribution across human atria (Li et al. 2000). Different inter-atrial distributions of  $I_{\text{K}}$  may have a functional role in the maintenance of re-entry arrhythmias (Li et al. 2000). Gintant (1995) demonstrated transmural differences in  $I_{\text{K}}$  current densities that are associated with longer APDs in mid-myocardial cells of dogs as compared to epi- and endocardial cells. In guinea pigs, ventricular subepicardial myocytes and M-cells exhibit the longest and shortest APD<sub>90</sub> values and the lowest and highest  $I_{\text{K}}$  densities, respectively (Main et al. 1998). Expression of  $I_{K_{\text{ur}}}$  in dogs is limited to atrial tissue and may therefore be responsible for shorter APD observed in canine atrium versus ventricle (Yue et al. 1999).

Due to the strong rate-dependent activation and inactivation kinetics displayed by  $K_{\text{v}}$  channels and the heterogeneity of  $K_{\text{v}}$  channel distribution within the myocardium, the combined effect of  $K_{\text{v}}$  channel expression and function on AP morphology will vary considerably under normal and abnormal conditions and between species and are therefore difficult to translate into specific effects on the ECG. However, differences in ECG morphology between species at rest under

normal conditions and under abnormal or diseased states do allow us to make some generalisations based on the difference in functional effects of  $K_V$  channels observed under experimental conditions.

Unfortunately atrial repolarisation is masked in the surface ECG by ventricular depolarization. However, effects of drugs and pathology on ventricular repolarisation can be mapped on the surface ECG through analysis of the J-T segment of the ECG. Under normal circumstances, direct reductions in  $K_V$ -mediated current are expected to prolong ventricular repolarisation and thereby produce a prolongation of the QT and J-T segments of the ECG. There is also an increase in the height of, and area under, the T-wave and possibly production of an abnormal T-wave morphology. Guo et al. (2000) have demonstrated that transgenic mice expressing homozygous dominant negative  $K_{V4.2}$  and  $K_{V1.4}$  subtypes of  $I_{to}$  exhibit rate-dependent prolonged ventricular AP and QT intervals and also exhibit spontaneous ventricular tachyarrhythmias. These same authors demonstrated that  $K_{V1.4}$  elimination alone had no significant effect on QT interval duration and that  $K_{V4.2}$  alone and in combination with  $K_{V1.4}$  elimination had profound effects on QT interval duration, thereby suggesting that compensatory upregulation of  $I_{to}$  subtypes may occur and thereby act as a limiting factor to excessive QT interval prolongation. In a mouse model of the Jervell and Lange-Nielsen syndrome in which a double homozygous loss-of-function mutation in *KCNQ1* is introduced, animals exhibit the three characteristics described above (Casimiro et al. 2001). It should be recognised that *KCNQ1* was the first member of the *KCNQ* family of  $K^+$  channels that are structurally similar to  $K_V$  and is identified as the gene responsible for the long QT syndrome, LQT1. Thus, under relatively defined conditions, reductions in  $K_V$  channel function and expression have potentially predictable effects on APD and the ECG.

It should be appreciated by safety pharmacologists that as the NCE drug concentration increases in the model or plasma, cellular effects become less defined due to the complex interactions between the NCE and many ion channels, their multiple subtypes and activation of compensatory and adaptive physiological mechanisms. Under these circumstances, the expression and function patterns of a single ion channel group or subgroup may not produce the predicted macroscopic effects as measured by either the AP or ECG. For example, both  $I_{to}$  and  $I_K$  are reduced (>50 %) in chronic and postoperative atrial fibrillation and both disorders are marked by reduced atrial APD and atrial ERP (AERP) and maintained re-entry, a consequence of AF-induced remodelling. An understanding of the properties of the ion channels involved would suggest that reductions in these currents should produce an anticipated contradictory effect. That is, APD prolongation and an increase in AERP followed by an increase in re-entry path length and abolition of the arrhythmia should result. However, in reality the reductions in  $I_{to}$  and  $I_K$  probably do serve as protective measures but are impeded in their efforts by changes in other ion channel function. It is known that a reduction in  $I_{Ca}$  may be greater than the overall reduction in  $I_K$  in atrial fibrillation (AF) and therefore may have a greater impact on APD and AERP reductions associated with chronic and postoperative AF. This concept has been reiterated by work in dogs that shows that

reductions of up to 75 % of atrial  $I_{to}$  current could not compensate for reductions in  $I_{Ca}$  associated with AF and remodelling (Yue et al. 1997). However, the effects described above appear to be very specific for AF secondary to  $Ca^{2+}$  overload-induced hypertrophy and the physical act of remodelling under the influence of the arrhythmia. Therefore, location and distribution of  $K_V$  channels and their interactions with other ion channel families may have important implications for specific diseased states, pharmacological management and safety.

Heart failure, hypertrophic cardiomyopathy and myocardial infarction are just several of the cardiac disorders associated with prolonged and abnormal QT intervals of the ECG and region-specific reductions in  $I_{to}$  and  $I_K$  with subsequent increases in APD (Yue et al. 1997). Reductions in  $I_{to}$  may lead to the improper establishment of the plateau of the cardiac AP and to subsequent changes in  $Ca^{2+}$  ion release and loading that result from changes in L-type  $Ca^{2+}$  channels,  $I_{Ca,L}$ , and  $Na^+-Ca^{2+}$  exchange, effective mechanisms that increase the inotropic capability of the myocardium in the diseased state (Yue et al. 1997). Reduced  $I_K$  may also be responsible for improper plateau phase repolarisation of the AP with subsequent effects on the late phase of repolarisation mediated by inwardly rectifying  $K^+$  ( $I_{Kir}$ ) channels and hence prolongation of the AP and the QT interval of the ECG. Together these two effects may manifest themselves as early and/or late afterdepolarisations and the arrhythmias associated with them (Studenik et al. 2001).

Interestingly, Han et al. (2000) have explored  $K^+$  channel heterogeneity and shown that canine Purkinje fibres express  $I_{to}$  currents that are functionally and pharmacologically different from ventricular  $I_{to}$  currents. Clinically, such heterogeneity also exists in  $I_{to}$  current.

The best characterised of the cardiac disorders involving a  $K^+$  channel is the long QT syndrome (LQTS), the clinical effect that ushered in the discipline of SP over a decade ago. It is a specific cardiac disorder that is related to genetic alterations (either acquired or inherited) or occur due to drug blockade of the  $I_K$  channel. Regardless of the cause, it results in the development of a specific, distinguishable, cardiac phenotype called torsade de pointes or TdP. While a number of genetic loci (such as 11p15 in humans) have been identified that contain the genes responsible for LQTS, the majority of these loci encode  $\alpha$ - and  $\beta$ -subunits for the  $I_K$  channel (Roberts and Brugada 2000).

In most mammalian species, a gene from the KCNQ (formerly  $K_VLQT$ ) subfamily, KCNQ1, when co-expressed with the auxiliary subunit, minK (or IsK or KCNE1), combines to form functional  $K^+$  channels that mimic the slowly activating component of the delayed rectifier current ( $I_{Ks}$ ). LQTS1 is associated with abnormalities in both of these potassium channel subunits and is expressed as auditory and cardiac phenotypes in the Jervell and Lange-Nielsen syndrome (Casimiro et al. 2001). Using site-directed mutagenesis, Hoppe et al. (2001) have determined that mutations in the human *ether-a-go-go* (*Eag*) related gene (HERG) can suppress  $I_{Kr}$  and lead to significant transmural variability in beat-to-beat APD and ECG morphology. Also, KCNE1 mutagenesis can markedly suppress  $I_{Ks}$  and result in the development of early afterdepolarisation arrhythmias (EADs). Thus, delayed repolarisation predisposes the heart to EADs and provides a mechanism for

functional block resulting in the maintenance of a polymorphic re-entry pattern due to APD heterogeneity and potential for induction of TdP.

The association of HERG (Erg1 or KCNH2 gene) with minK (KCNE1) or KCNE2 (a minK homolog called MiRP) forms the molecular equivalent of the rapidly activating delayed rectifier  $K^+$  channel ( $I_{Kr}$ ) (Nerbonne 2000). Missense and frameshift mutations in a number of locations within the HERG  $\alpha$ -subunit have been demonstrated and proposed as possible mediators of LQTS2; however, mutations in the KCNE2  $\beta$ -subunit have been less numerous and have not been implicated in LQTS2 (Roberts and Brugada 2000). Mutations in the HERG sequences responsible for inactivation (both N- and C-type) and mutations within the pore loop alter the kinetics of  $I_{Kr}$  channels. These mutations, or equally they could be sites in which an NCE may interact, could potentially be associated with drug-induced LQTS2 and result in an increased tendency to development of cardiac arrhythmias.

The development of potent and selective methanesulfonamide drugs led to the discovery of an unexpected adverse event in the form of pronounced QT prolongation at low heart rates and induction of TdP. Subsequent studies indicated that the methanesulfonamide group of drugs were also potent blockers of native  $I_{Kr}$  channels in cardiac tissue as well as the molecular correlate of  $I_{Kr}$ , the HERG  $K^+$  channels. Since they were potent blockers of these channels, they could essentially produce a chemical loss-of-function type of mutation. This uniform chemical loss-of-function type of mutation, if it occurs across a background of non-uniformly distributed  $K_V$  channels within the myocardium, may suggest a potential mechanism whereby these types of cardiac drugs (as well as the plethora of non-cardiac drugs that produce QT interval prolongation) produce a dispersion of refractoriness and a predisposition to TdP (Nalos et al. 2012). Drug-induced long QT syndrome developed into a major concern for the pharmaceutical industry, as well as global regulatory authorities since a wide range of non-cardiac marketed drugs (beginning with terfenadine) unexpectedly prolonged the QT interval precipitating TdP in patients. Terfenadine, a clinically used, non-sedating histamine ( $H_1$ ) receptor antagonist, was the first drug to be shown to block HERG channels (Roy et al. 1996). Thus as a result of the effects of non-cardiac drug block of HERG ion channels and the involvement of these same channels in TdP arrhythmias and sudden cardiac death led to development of the regulatory requirements that appropriate safety studies be conducted in which this aspect of channel block and effects on the ECG be determined, the remit of SP.

### 7.3 The Inward Rectifier Potassium Current ( $I_{Kir}$ )

The inward rectifier ( $K_{ir}$  or  $I_{K1}$ )  $K^+$  channel can be described mathematically with a single gate that operates so fast (usually less than a ms) that  $g_{K1}$  can be treated as changing instantaneously with voltage; since channels close with depolarisation, there is in effect a *very* strong inward rectification. The inward rectification of these channels tends to hold the resting membrane potential close to  $V_K$ . These channels



are greatly dependent on  $K^+$  and this probably accounts for the strong dependence of myocardial cell excitability on  $K^+$ .

The  $K_{ir}$  channel  $\alpha$ -subunits have been defined and, like other  $K^+$  channels, are widely distributed in the mammalian genome. More than 15  $\alpha$ -subunits have been defined and grouped into seven families ( $K_{ir}1$ –7). The  $K_{ir}2$ ,  $K_{ir}3$  and  $K_{ir}6$  families appear to be the most important with respect to  $K^+$  channel function in the mammalian myocardium. Within the  $K_{ir}2$  family, the genes for subunits  $K_{ir}2.1$ , 2.2 and 2.4 combine to form  $I_{K_{ir}}$  (Topert et al. 2000) while the  $K_{ir}3.1$ –3.4 subunits form G-protein-coupled inward rectifying  $K^+$  channels ( $I_{KACH}$ ) (Sakura et al. 1995). The ATP regulated inward rectifying potassium channels ( $I_{KATP}$ ) are formed from  $\alpha$ -subunits produced by genes for  $K_{ir}6.1$  and 6.2 (Ashcroft and Gribble 2000).

### 7.3.1 Molecular Genetics of $I_{K_{ir}}$

The  $K_{ir}$  channels exhibit the simplest structure of all of the  $K^+$  channel families (see Fig. 5) described to date comprised of the most basic form of a  $K^+$ -selective pore and possibly the evolutionary starting point for  $K_V$  and  $K_{2P}$  channel formations (Nerbonne 2000). The pore-forming  $\alpha$ -subunits exhibit two transmembrane-spanning sequences with a pore loop sequestered between them and intracellular N- and C-terminals. However, the sulfonylurea receptor (SUR) accessory subunits that combine with the  $\alpha$ -subunits to form functional channels exhibit extracellular and intracellular N- and C-termini respectively and 17 transmembrane-spanning sequences in a 5-6-6 configuration (Ashcroft and Gribble 2000). Like the  $K_V$  and  $K_{2P}$  channels, functional  $K_{ir}$  channels are formed through the oligomeric association of  $\alpha$ - and accessory subunits to form the  $K^+$ -selective pore-forming region. However, unlike these channels, some of the  $K_{ir}$  channels (such as  $I_{KATP}$  in pancreatic  $\beta$ -cells) only exist as functional channels in an octomeric form. The octomeric form results from the association of 4  $K_{ir}$  subunits with 4 SUR subunits as opposed to typical functional tetramers. These functional  $K_{ir}$  channels then require homooligomerisation of subunits where 4  $K_{ir}6.2$  subunits and 4 SUR1 subunits co-assemble as opposed to hetero-oligomerisation (Ashcroft and Gribble 2000). The H5 loop of  $K_V$  channels and the signature sequence G(Y)G selectivity filter of the pore are found in all  $K_{ir}$  channels. Unlike the  $K_V$  channels,  $K_{ir}$  channels lack an intrinsic S4 voltage-sensing element and a mechanism for rapid N-type inactivation and therefore do not 'sense' and respond to changes in membrane potential in the manner of  $K_V$  channels. The  $K_{ir}$  channels are nonetheless affected by membrane voltage. The orientation of the M2 transmembrane-spanning sequences is believed to provide the permeability filter whereas M1–M2 orientation relative to each other is believed to provide the channel gating mechanism (Ashcroft and Gribble 2000). However, due to their early evolutionary appearance (e.g. as KcsA in some bacteria) and abundance in primitive intracellular structures (e.g. mitochondria), most  $K_{ir}$  channels play large roles in linking cellular metabolism to excitability.

### 7.3.2 Functional and Pharmacological Properties

Within the heart,  $I_{K1}$ ,  $I_{KATP}$  and  $I_{KACH}$  play different roles due to their unique functional properties and channel distributions.  $I_{K1}$  is strongly active at potentials



close to the resting membrane potential; therefore,  $I_{K1}$  plays an important role in the maintenance of the AP plateau, rapid terminal repolarisation and resting membrane potential. Both  $I_{KATP}$  and  $I_{KACH}$  are ligand-gated currents and are therefore heavily regulated by both intracellular and extracellular messages.  $I_{KATP}$  is regulated by myocardial metabolic status and those elements that serve key functional roles in metabolism (e.g. glucose, ATP/ADP,  $CO_2$  and pH) (Weiss and Venkatesh 1993). Therefore  $I_{KATP}$  will have a strong functional role in the regulation of cardiac excitability under both normal and abnormal conditions (e.g. ischaemia or infarction).  $I_{KACH}$  is sensitive to G-protein regulation in both a muscarinic (M) receptor dependent and independent manner and is therefore susceptible to modulation via the autonomic nervous system and by a variety of other G-protein-coupled receptor systems. As such,  $I_{KACH}$  is instrumental in vagal mediated heart rate modulation and beat-to-beat management during exercise and other physiological situations where rapid changes in heart rate occur.

Like most  $K^+$  channels, the  $K_{ir}$  channels extrude intracellular  $K^+$  in order to re-establish the membrane potential and to bring about cellular repolarisation in excitable myocardial cells. Therefore, activation of  $K_{ir}$  channels is expected to increase APD whereas a reduction of this current is expected to increase APD. An increase in  $I_{K1}$  is associated with a reduction in the J-T segment duration and a narrowing of the T-wave in the ECG. Wu et al. (1999) showed that  $I_{K1}$  blockade in the rabbit heart, with concomitant APD and  $QT_c$  prolongation, is associated with an almost complete flattening of the T-wave in accordance with the known relationship between T-wave amplitude and activation time. Interestingly, the same authors showed that  $I_{K1}$  blockade had a greater effect on T-wave morphology than did  $I_{to}$  blockade, thereby demonstrating the relative importance of the two  $K^+$  channel types in rabbit ECG morphology. Additionally, blockade of  $I_{K1}$  with  $Ba^{2+}$  produced increases in the APD of both atrial and ventricular myocytes and prolonged the rate-corrected QT interval of isolated rabbit hearts without detrimental effects on conduction and no proarrhythmic potential (Wu et al. 1999). It was a result of these properties that drugs such as terikalant (RP58866) were investigated for their antiarrhythmic potential (Rees and Curtis 1995). Williams et al. (1999) have shown that  $I_{K1}$  is involved in the rate-dependent shortening of APD and that terikalant possesses positive rate-dependent prolongation of the AP, a unique profile compared to selective blockers of the  $I_K$  channel. Wu et al. (1999) have shown that terikalant maintains its ability to prolong APD at depolarised membrane potentials and abolish ischaemia-induced arrhythmias. However, terikalant also produces significant inactivation block of HERG and theoretically could predispose the heart to idiopathic LQTS and TdP arrhythmias. Farkas and Coker (2002) evaluated terikalant in a proarrhythmia model and showed that it produced limited induction (20 %) compared to clofilium (60 %). Due to the nature of  $I_{K1}$  activation and role in rate-dependent APD modification, drugs that selectively block  $I_{K1}$  were initially hoped to provide antiarrhythmic efficacy. Development of the class has halted.

The pharmacology of  $I_{KATP}$  channels has been very well studied. Briefly, sulfonylurea drugs such as glibenclamide bind with high affinity to the sulfonylurea receptor (SUR1) subunit and produce blockade of  $K_{ATP}$  channels. Diazoxide as well

as benzopyran derivatives such as cromakalim also bind to SUR1 but act to open  $K_{ATP}$  channels (Ashcroft and Gribble 2000). The role of  $I_{KATP}$  openers in the treatment of atrial and ventricular arrhythmic disorders is limited due to the drug's potential to reduce APD and thereby predispose cells to maintenance of re-entry circuits. However, in situations where bradycardia and much slowed conduction are associated with depressed myocardial function, the administration of  $I_{KATP}$  openers may be of use in reversing the depressive state. The role of  $I_{KATP}$  blockers on the other hand is much less clear. In some models  $I_{KATP}$  blockade by glibenclamide produces antiarrhythmic protection whereas in others the protection is either limited, not apparent and even detrimental (Barrett and Walker 1998). Like most of the  $K^+$  channel pharmacology described in this chapter, the effects of  $I_{KATP}$  blockade by an NCE (or augmentation in myocardial disorders) will depend specifically on the role of the  $I_{KATP}$  channel in off-target drug activity and the selectivity of drugs with which  $I_{KATP}$  can be augmented in cardiac disorders. As a result of the strong link between  $I_{KATP}$  channels and cellular metabolism, these channels may be expected to have a limited, discernible contribution to the ECG under normal circumstances. However, these same channels might be expected to contribute significantly to observed changes in ECG morphology in diseased or metabolically compromised states.

The pharmacology of  $I_{KACH}$  is at least as diverse as the substantial pharmacology of G-proteins and the numerous receptors and intracellular signals that modulate these channels and will therefore not be discussed in detail here.  $I_{KACH}$  is highly expressed in atria and in particular the SA node. Less expression is found within the ventricles, in agreement with the fundamental role of this channel in autonomic regulation of heart rate and, therefore, may be significantly affected by pharmacological manipulation of atrial or SA node cells. The effects of  $I_{KACH}$  on APD and the ECG may be observed most readily through analysis of A-H and H-V cardiac electrograms since the channel may have very little influence on ventricular repolarisation.

Previously we described the regulation and function of  $K_V$  channels in AF (see  $K_V$  section above) and the apparent paradox that exists whereby a reduction in  $K_V$  channel density occurs with a reduced APD in AF following remodelling in the heart. This physiological effect is similarly relevant to consideration of drug effects in the ventricle. The  $I_{K1}$  channel may also play a role in APD reduction during AF-induced remodelling in addition to the effects of a reduced  $I_{Ca}$  and in keeping with its strong function in rate-dependent APD shortening (Farkas and Coker 2002). Bosch et al. (1999) have demonstrated that increases in both  $I_{K1}$  and  $I_{KACH}$  densities in AF remodelled human atria, along with reduced  $I_{Ca}$ , may circumvent the protective reductions in  $K_V$  currents exhibited. Therefore, selective pharmacological manipulation of  $I_{K1}$  and/or  $I_{KACH}$  with drugs such as adenosine is useful in the treatment of supraventricular arrhythmias such as AF.

## 8 The Electrocardiogram

Electrical activity in electrically excitable cells results from the opening and closing of ion channels in a voltage- and time-dependent manner. The depolarisation of a single cardiac cell results in the electronic spread of electrical activity to adjacent cells and the production of current which flows in the direction of depolarisation. A second, repolarising current, is established in order to restore electrical excitability to cells. If these currents are recorded in individual cells we observe an AP, if they are recorded on the surface of the body we observe an electrocardiogram (ECG).

Thus, the electrocardiogram (ECG) is most easily defined as the global summation of all the electrical activity that is generated by cells within the various regions of the heart. It represents the rate of change of voltage across all the cell membranes as a function of time,  $\Delta V_m/dt$ . Willem Einthoven first developed the ECG in 1903 (Einthoven 1912). It was realised early on in its development that components of the electrical signal coincide with components of electrical signals that arise within cardiac muscle. These ECG intervals represent activation and inactivation properties of the myocardial cells.

The intervals that are defined by the ECG present both the clinician and safety pharmacologist with a fundamental tool with which to diagnose disease or investigate drug safety and elucidate mechanisms responsible for ECG changes that could suggest development of aberrant electrical activity (i.e. arrhythmia) within the heart. The ECG is a sensitive enough diagnostic tool to delineate drug-induced changes in electrical activity or diseases such as regional myocardial infarction or cardiac hypertrophy or can provide indications of abnormal electrolyte levels.

Within conducting tissue, there exists an important cellular hierarchy which ensures proper genesis and conduction of current and hence contraction of cardiac muscle since all cells in the heart are capable of generating electrical impulses spontaneously. Thus, under some conditions, various cells in the heart can display the property of automaticity. The sino-atrial node (SAN) dominates and is the primary pacemaker of the heart, as it possesses the highest rate of automaticity compared to any other cell in the heart. Electrical impulses generated by cells within the SAN are conducted across atrial conduction pathways, through the AV node (AVN) into the bundle of His. The impulse then moves down the left and right bundle branches into Purkinje fibres that are diffusely spread throughout the myocardium and terminate in muscle cells. The propagation of an electrical impulse generated in the SAN through cardiac tissue is proportional to the volume of tissue that is electrically excitable. Hence, the various deflections observed in the ECG waveform also reflect the changing size of the tissue that is generating and conducting the current.

Electrical activity generated by atrial depolarisation is recorded on the ECG as the P-wave. Atrial repolarisation occurs immediately, as the ventricles depolarise; however, since the ventricular depolarisation occurs at the same time, the repolarisation wave for the P-wave of the atria is not observed on the ECG. Rather, a large QRS complex is observed to follow the P-wave. Ventricular depolarisation is a composite of the Q, R and S waves. The Q-wave represents depolarisation of the

interventricular septum, while the R-S complex represents the simultaneous depolarisation of both the left and right ventricles. Due to the dissimilarity in muscle mass between the ventricles, the QRS complex, by convention, represents depolarisation of the left ventricle. Repolarisation of the ventricles is recorded on the ECG as the T-wave. Occasionally a U-wave is present in the ECG (as slow heart rates) which represents the final stages of ventricular repolarisation. It usually results from repolarisation of papillary muscles or ventricular septum and occurs after most of the ventricular tissue has repolarised. In addition to waves and complexes, the ECG contains intervals and segments that represent flat or isoelectric sections on the ECG record.

The PR interval represents the time required for electrical impulse conduction from its origin at the onset of atrial depolarisation through the atrial conduction system to the ventricular myocardium. It generally represents conduction time across the AVN. Changes in this interval, in most species, reflect changes in  $\text{Ca}^{2+}$  channel function; however, in the rat  $\text{Na}^+$  channels are dominant (Botting et al. 1985). Unlike the PR interval, the QT interval represents the ventricular refractory period and includes depolarisation and repolarisation of ventricular muscle. In contrast to the atria, the AP in ventricular tissue is long ( $\approx 300$  ms), which is a time interval that is similar to the duration of the QT interval. Thus, the QT interval is an approximate measure of ventricular repolarisation and thus  $\text{K}^+$  channel function.

Only three segments of the ECG will be discussed. The PR segment represents the time required for an electrical impulse to propagate from the AVN through to the ventricular myocardium. It reflects the time between the end of atrial depolarisation and the onset of ventricular depolarisation. The ST segment is one of the most important measures of the ECG since it represents the early phase of ventricular repolarisation. If a depression in this segment of the ECG occurs, it can be used to diagnose conditions whereby a reduction in coronary blood flow occurs to the heart. An elevation in this segment occurs in a damaged area to the ventricular wall that may be associated with myocardial ischaemia or infarction. However, any abnormality in these measures may be indicative of some underlying pathophysiological process that alters the AP in cardiac cells that are a consequence of changes in voltage-gated ion channel(s) in tissue. Note that if the ST segment of the ECG is absent, the T-wave is thought of as beginning at the end of the QRS complex, or the J-point. Most often a J-T interval can be measured as the distance from the convergence of the J-point and the isoelectric baseline to the end of the T-wave (i.e. where the T-wave returns to the isoelectric line). However, sometimes the onset and end of the T-wave are difficult to determine. This measure provides a representation of ventricular repolarisation independent of the QT interval and is sometimes used as an indirect assessment of the heterogeneity of repolarisation.

Since the ECG is a composite of many voltage-gated ion channels, it may not be consistent between various animal species. The variability may be quantitative, i.e. different currents or current densities in the hearts of different species may result in differences in the duration of various segments or intervals. The variability may also be qualitative, i.e. the ECG may exhibit a different shape as a result of the

expression of an ion channel distinct from that found in the human heart or in other species.

These marked variations can be observed in the ECGs from animals and are especially noticeable when compared to ECGs recorded in humans. While little disparity exists regarding the role of both  $\text{Na}^+$  and  $\text{Ca}^{2+}$  channels in the hearts of various species, the rat being an exception, important species and regional differences exist in the contribution  $\text{K}^+$  channels make to repolarisation of the cardiac AP. Studies have shown that electrophysiological distinctions can be made between epi- and endocardial tissue in many species including the dog (Yan et al. 1998). In canine ventricles, epicardial, mid-myocardial (M-cells) and endocardial cells display distinct electrical properties and hence different AP morphology (Antzelevitch 2004). Wang et al. (1998) have characterised epicardial and endocardial differences in APD in human atrial tissue and suggest that the ionic mechanism for these differences is due to different amplitudes of the transient outward  $\text{K}^+$  current ( $I_{\text{to}}$ ). Similar differences are also seen in ventricular tissue. In the rat the density of the fast component of  $I_{\text{to}}$ ,  $I_{\text{to,f}}$ , current is greater in the atria than in the ventricle while in the mouse the opposite is observed (Nerbonne 2000). However, this current is ubiquitous in the hearts of most species including humans, rat, mice, feline, canine and ferrets. Not unlike  $I_{\text{to,f}}$ , other  $\text{K}^+$  current densities vary in myocardial cells. The delayed rectifier ( $I_{\text{K}}$ ) current is greater in the atria than in the ventricles of the guinea pig (Sanguinetti and Jurkiewicz 1991). Thus, the disparity in level of  $\text{K}^+$  channel expression and the resulting current density contribute significantly to the variations in AP waveforms observed in myocardial cells in the atria and ventricles and in turn result in differences in the recorded ECG.

The diversity of ion channels present in cardiac tissue has been observed, to a greater degree than by simply recording currents from whole and isolated cardiac tissue, through molecular cloning procedures. The molecular cloning of various ion channels, their component current subtypes and accessory subunits has resulted in the establishment of an even greater level of ion channel diversity than could have originally been anticipated. The complexity in ion channels arises from the diverse protein nature of the individual pore-forming  $\alpha$ -subunits present in cardiac tissue and also as a result of alternative splicing of transcripts for these proteins. The large number of accessory subunits specific for the ion channel again complicates matters.

## 8.1 ECG Changes that Can Occur in the Myocardium

The ECG can be used as a means to detect cardiac related adverse drug effects or as a diagnostic aid for disease since many of its intervals and segments are sensitive to electrical, biochemical and pathological changes in myocytes. In humans, common causes of arrhythmias include myocardial ischaemia, myocardial infarction or reperfusion of a previously ischaemic myocardium. These conditions can be readily reproduced in both intact and isolated hearts in many species. While the pathology of arrhythmias may not appear to be relevant to the safety pharmacologist, the

mechanism(s) derived from arrhythmia studies that explain arrhythmogenesis have direct implications in the development of the CIPA paradigm and its ability to assess the 'proarrhythmia potential' for a new drug. The mechanism(s) developed will be important in the interpretation of ion channel binding data and predicted changes in the AP using *in silico* models. Thus, a review of the pathological changes associated with the ischaemic myocardium is warranted since an understanding of such changes is likely to better arm the safety pharmacologist when drug-mediated adverse cardiac effects produce altered depolarisation (PR and QRS interval) and repolarisation (QT or T-wave morphology) effects.

The hearts of many non-clinical species used in SP studies including primates, pigs and rats do not have extensive coronary collaterals, i.e. these coronary arteries are end-arteries, like humans (Schaper et al. 1986). Thus, when a coronary artery is occluded an area is rendered uniformly ischaemic. If occlusion of an artery persists, irreversible damage occurs and progresses until infarction results. The time dependency of the onset of arrhythmias after occlusion is characteristic for many species. For example, arrhythmias first occur in conscious chronically prepared rats 5–15 min after occlusion during the reversible stage of ischaemia (Clements-Jewery et al. 2007). The most common arrhythmias seen include premature ventricular contractions (PVC), ventricular tachycardia (VT) and ventricular fibrillation (VF). A second arrhythmic period occurs 1–3 h after occlusion during the evolution of the infarct and consists of PVC, VT and VF (Clements-Jewery et al. 2007). Various factors influence the severity and incidence of arrhythmic outcomes after occlusion. These include both the size of the ischaemic zone and the serum  $K^+$  concentration.

Well-defined ECG changes commonly occur in many animal models of coronary artery occlusion. These time-dependent changes delineate the course of events associated with ischaemia. Typically, occlusion of a coronary artery results in a change in the R-wave amplitude that begins within minutes after occlusion followed by an elevation in the S–T segment and many types of arrhythmias including VT and VF. The mechanism by which S–T segment elevation occurs is not known but is suggested to relate to changes in cellular biochemistry and electrophysiology (possibly due to ion channels' up- or downregulation) as they relate to anoxia and deranged energetics. ECG responses to ischaemia are well defined in many animal species.

Ischaemia also produces changes in the extracellular milieu of the cell. Case et al. (1979) showed that ischaemia increases extracellular  $K^+$  and is accompanied by changes in pH,  $O_2$  and  $CO_2$  levels within the ischaemic zone. These changes in ion concentrations have become better defined with improved experimental techniques including ion-sensitive electrodes, nuclear magnetic resonance (NMR) and voltage-sensitive dyes.

Briefly, the intracellular events that occur as a result of ischaemia includes a reduction in pH, an elevation in  $Na^+$  due to partial suppression of the  $Na^+/K^+$ -ATPase pump and an increase in  $Ca^{2+}$ . Many of these changes are not homogeneous within the ischaemic myocardium due to local variations in accumulation and diffusion of cellular wastes such as  $CO_2$ . This may have implications in the changes observed in the ECG since ion channel properties change as well as in the

development of arrhythmogenic circuits (see below). Accompanying the intracellular changes are extracellular changes. Within the ischaemic myocardium, there is a triphasic increase in  $K^+$  which, unless reversed, results in an irreversible loss in membrane integrity (Hill and Gettes 1980). A reduction in extracellular pH occurs that parallels the change in extracellular  $K^+$  levels. In a similar manner, intracellular events are varied and contribute to the heterogeneity within ischaemic tissue. In addition to the local micro-inhomogeneities of ions which occur within the myocardial extracellular space, Hill and Gettes (1980) also showed that a disparity exists between the centre and the border zone of the developing ischaemic tissue and still yet between the myocardial subepicardium and subendocardium. These transmural differences have been associated with the wave-like spread of ischaemia from the endocardium to the epicardium.

Abnormal impulse generation can arise from oscillations in the membrane potential and has been characterised as triggered rhythms (Binah and Rosen 1992). These triggered rhythms occur in two forms: early or late afterdepolarisations (EADs or DADs).

## 8.2 Early Afterdepolarisations

EADs interrupt either Phase 2 or 3 repolarisation of the AP. If these afterdepolarisations attain sufficient thresholds, they may produce triggered responses and induce single or multiple extrasystoles and even VT. The EAD is an oscillatory potential that is sensitive to frequency and often occurs at slow stimulation rates. EAD activity has been shown in vitro using many types of isolated cardiac muscle and various cell types including mid-myocardial cells (M-cell) (Antzelevitch 2004). Induction of EAD activity can be induced by a variety of drugs that block sodium and potassium channels as well as by catecholamines.

The ionic basis for EAD development is unclear. However, studies suggest the involvement of the slow inward  $Ca^{2+}$  current ( $I_{si}$ ) of the cardiac L-type  $Ca^{2+}$  channel during the plateau of the AP. Essentially,  $I_{si}$  re-activation acts as a depolarising charge carrier during the depolarising phase of the EAD. Prolongation of the plateau phase of the AP allows for an increased time for  $Ca^{2+}$  channel recovery which enhances the inward current, thereby depolarising the membrane and sustaining the EAD. Other proposed mechanisms include a reduction of outward  $K^+$  currents resulting in slow repolarisation and an increase in  $Na^+$  window current associated with a prolonged plateau of the AP. Ultimately, arrhythmias which result include the long Q-T syndrome and TdP; however, the genesis and maintenance of these arrhythmias by an EAD mechanism remain unclear.

## 8.3 Delayed Afterdepolarisations (DADs)

Transient depolarisations that occur during Phase 4 of the cardiac AP are dependent upon the rate of the preceding AP (Antzelevitch and Sicouri 1994). Unlike EADs



the amplitudes of DADs increase with decreasing cycle lengths. DADs have been observed under a variety of experimental conditions all of which have a similar end result, i.e. intracellular  $\text{Ca}^{2+}$  overload. High intracellular  $\text{Ca}^{2+}$  concentrations saturate sarcoplasmic reticulum sequestration mechanisms resulting in  $\text{Ca}^{2+}$  oscillations due to  $\text{Ca}^{2+}$ -induced  $\text{Ca}^{2+}$  release (Clusin 2003). The ionic currents that contribute to this mechanism are not known. Ischaemia, digitalis and catecholamines can directly produce DAD by enhancing  $\text{Ca}^{2+}$  entry into cells. Thus,  $\text{Ca}^{2+}$  channel blockers, such as verapamil, abolish DADs. Studies show that  $\text{Na}^+$  channel blockers including lidocaine and the  $\text{K}^+$  channel activator, pinacidil, may all effectively suppress DAD and DAD-induced triggered activity (Clusin 2003).

#### 8.4 Re-entrant Arrhythmia Pathways

The major cause of ventricular arrhythmias is due to re-entry. Re-entry has been subdivided into either circus-movement excitation or reflection (Wit and Rosen 1983). The basic model for re-entrant circus movement is a bifurcating Purkinje fibre bundle attached to the ventricle that gives rise to different anatomical conduction pathways. Re-entry occurs when antegrade conduction of the impulse is extinguished at a site of unidirectional block. This type of block may arise from ischaemic damage of previously normal conduction pathways. If normal conduction continues in the other branches of the pathway, an impulse can retrogradely enter the area of unidirectional block where its conduction is slowed but not extinguished. The impulse can then emerge from this depressed area and, providing that the cells are not refractory, re-excite the tissue proximal to the area of block. This generates premature ventricular complexes (PVC) which can remain as such, or deteriorate into VT or VF along a pre-existing pathway and usually results in VT. Random re-entry of impulse propagation results when electrophysiological differences exist between areas of cardiac muscle. The development of ischaemia in cardiac muscle is a dynamic process; therefore, the pathway is not constant for the impulse which circulates. It may fractionate, produce multiple re-entrant circuits and result in VF.

The mechanisms suggested for arrhythmogenesis are complex and all, under ischaemic conditions, may play a significant role. It is most likely that re-entry dominates during VT and VF while the mechanisms for PVCs are less clear. However, the changes observed in the ECG under these conditions provide a reliable index of myocardial ischaemia; further studies in the area of ion channel physiology, molecular biology and how ion channels change during conditions of ischaemia may provide us the fundamentals for novel therapeutic drug development.



## 9 Conclusion

Thus, SP continues to seek to provide validation and refine methods for use in preclinical hazard detection of NCE adverse effect liability. It does so in accordance with the scientific methods that rapidly progress with technology advances for functional measures. Additionally, while SP seeks to organise the strategy of implementation of methods according to regulatory guidance documents issued by the ICH and regulatory authorities, it aims to maximise translational value of the data acquired in hope of better predictivity in drug development. Currently there is an evaluation ongoing that thinks ‘outside the box’ with regard to characterising the safety profile of novel drugs in development. The CIPA initiative seeks to provide a greater comprehensive assessment of the direct proarrhythmic potential of a drug. It is hoped that implementation of this assay which focuses on the evaluation of multiple cardiac ion channels can be ultimately developed to assess drug effects on human cardiac electrophysiology with perhaps induced pluripotent stem cells acting as the validated, sensitive and specific cellular assay. Implicit understanding is required of basic ion channel biophysics and cardiac electrophysiology of sodium, calcium and potassium channels that constitute the AP and arrhythmia mechanisms. Thus, the paradigm shift related to CIPA is being realised by safety pharmacologists and because of this the discipline remains in evolution and this coverage of new aspects of safety is certain to expand to provide better, or modified, guidance in the next few years.

---

## References

- Aldrich RW, Corey DP, Stevens CF (1983) A reinterpretation of mammalian sodium channel gating based on single channel recording. *Nature* 306:436–441
- Anon (2001) ICH S7A: Safety pharmacology studies for human pharmaceuticals. Fed Regist 66:36791–36792. Retrieved January 2015 at: <http://www.fda.gov/downloads/Drugs/GuidanceComplianceRegulatoryInformation/Guidances/ucm074959.pdf>
- Anon (2005) ICH S7B: The nonclinical evaluation of the potential for delayed ventricular repolarization (QT interval prolongation) by human biopharmaceuticals. Fed Regist 70:61133–61134. Retrieved January 2015 at: <http://www.fda.gov/downloads/Drugs/GuidanceComplianceRegulatoryInformation/Guidances/ucm074963.pdf>
- Antzelevitch C (2004) Arrhythmogenic mechanisms of QT prolonging drugs: Is QT prolongation really the problem? *J Electrocardiol* 37:15–24
- Antzelevitch C, Shimizu W (2002) Cellular mechanisms underlying the long QT syndrome. *Curr Opin Cardiol* 17:43–51
- Antzelevitch C, Sicouri S (1994) Clinical relevance of cardiac arrhythmias generated by after-depolarizations. Role of M cells in the generation of U Waves, triggered activity and torsade de pointes. *J Am Coll Cardiol* 23:259–277
- Armstrong CM, Bezanilla F (1974) Charge movement associated with the opening and closing of the activation gates of the Na channels. *J Gen Physiol* 63:533–552
- Armstrong CM, Hille B (1998) Voltage-gated ion channels and electrical excitability. *Neuron* 20:371–380
- Armstrong CM, Bezanilla F, Rojas E (1973) Destruction of sodium conductance inactivation in squid axons perfused with pronase. *J Gen Physiol* 62:375–391

- Ashcroft FM, Gribble FM (2000) New windows on the mechanism of action of K(ATP) channel openers. *Trends Pharmacol Sci* 11:439–445
- Aubert M, Osterwalder R, Wagner B, Parrilla I, Cavero I, Doessegger L, Ertel EA (2006) Evaluation of the rabbit Purkinje fibre assay as an in vitro tool for assessing the risk of drug-induced torsades de pointes in humans. *Drug Saf* 29:237–254
- Authier S, Pugsley MK, Curtis MJ (2015) Hemodynamic assessment in safety pharmacology. In: Pugsley MK, Curtis MJ (eds) *Principles of safety pharmacology*. Springer, Heidelberg
- Barrett TD, Walker MJA (1998) Glibenclamide does not prevent action potential shortening induced by ischemia in anesthetized rabbits but reduces ischemia-induced arrhythmias. *J Mol Cell Cardiol* 30:999–1008
- Beatch GN, Abraham S, MacLeod BA, Yoshida NR, Walker MJ (1991) Antiarrhythmic properties of tedisamil (KC8857), a putative transient outward K<sup>+</sup> current blocker. *Br J Pharmacol* 102:13–18
- Bell RM, Mocanu MM, Yellon DM (2011) Retrograde heart perfusion: the Langendorff technique of isolated heart perfusion. *J Mol Cell Cardiol* 50:940–950
- Binah O, Rosen MR (1992) Mechanisms of ventricular arrhythmias. *Circulation* 85:I25–I31
- Bosch RF, Zeng X, Grammer JB, Popovic K, Mewis C, Kuhlkamp V (1999) Ionic mechanisms of electrical remodeling in human atrial fibrillation. *Cardiovasc Res* 44:121–131
- Botting JH, Curtis MJ, Walker MJA (1985) Arrhythmias associated with myocardial ischaemia and infarction. *Mol Aspects Med* 8:311–422
- Boyd PA, Hirose M, Dun W (2010) Cardiac Purkinje cells. *Heart Rhythm* 7:127–135
- Boyett MR, Harrison SM, Janvier NC, McMorn SO, Owen JM, Shui Z (1996) A list of vertebrate cardiac ionic currents nomenclature, properties, function and cloned equivalents. *Cardiovasc Res* 32:455–481
- Brack KE (2014) The heart's 'little brain' controlling cardiac function in the rabbit. *Exp Physiol*. doi:10.1113/expphysiol.2014.080168
- Case RB, Felix A, Castellana FS (1979) Rate of rise of myocardial pCO<sub>2</sub> during early myocardial ischemia in the dog. *Circ Res* 45:324–330
- Casimiro MC, Knollmann BC, Ebert SN, Vary JC Jr, Greene AE, Franz MR, Grinberg A, Huang SP, Pfeife K (2001) Targeted disruption of the *Kcnq1* gene produces a mouse model of Jervell and Lange-Nielsen Syndrome. *Proc Natl Acad Sci USA* 98:2526–25231
- Catterall WA (1980) Neurotoxins that act on voltage-sensitive sodium channels in excitable membranes. *Annu Rev Pharmacol Toxicol* 20:15–43
- Catterall WA (1993) Structure and function of voltage-gated ion channels. *Trends Neurosci* 16:500–506
- Catterall WA (1995) Structure and function of voltage-gated ion channels. *Annu Rev Biochem* 64:493–531
- Catterall WA (2001) A 3D view of sodium channels. *Nature* 409:988–991
- Cavero I, Crumb W (2005) ICH S7B draft guideline on the non-clinical strategy for testing delayed cardiac repolarisation risk of drugs: a critical analysis. *Expert Opin Drug Saf* 4:509–530
- Champeroux P, Viaud K, El Amrani AI, Fowler JS, Martel E, Le Guennec JY, Richard S (2005) Prediction of the risk of Torsade de Pointes using the model of isolated canine Purkinje fibres. *Br J Pharmacol* 144:376–485
- Chiu SY (1977) Inactivation of sodium channels: second order kinetics in myelinated nerve. *J Physiol* 273:573–596
- Clements-Jewery H, Curtis MJ (2014) The Langendorff preparation. In: Ardehali H, Bolli R, Losordo DW (eds) *Manual of research techniques in cardiovascular medicine*. Wiley Blackwell, Oxford
- Clements-Jewery H, Hearse DJ, Curtis MJ (2007) Neutrophil ablation with anti-serum does not protect against phase 2 ventricular arrhythmias in anaesthetised rats with myocardial infarction. *Cardiovasc Res* 73:761–769
- Clusin WT (2003) Calcium and cardiac arrhythmias: DADs, EADs, and alternans. *Crit Rev Clin Lab Sci* 40:337–375

- Coraboeuf E, Carmeleit E (1982) Existence of two transient outward currents in sheep cardiac Purkinje fibers. *Pflugers Arch* 392:352–359
- Corrias A, Giles W, Rodriguez B (2011) Ionic mechanisms of electrophysiological properties and repolarization abnormalities in rabbit Purkinje fibers. *Am J Physiol Heart Circ Physiol* 300: H1806–H1813
- Curtis MJ (1998) Characterisation, utilisation and clinical relevance of isolated perfused heart models of ischaemia-induced ventricular fibrillation. *Cardiovasc Res* 39:194–215
- Curtis MJ, Hancox JC, Farkas A, Wainwright CL, Stables CL, Saint DA, Clements-Jewery H, Lambiase PD, Billman GE, Janse MJ, Pugsley MK, Ng GN, Roden DM, Camm AJ, Walker MJA (2013) The Lambeth conventions (II): guidelines for the study of animal and human ventricular and supraventricular arrhythmias. *Pharmacol Ther* 139:213–248
- Darpo B, Garnett C, Benson CT, Keirns J, Leishman D, Malik M et al (2014) Cardiac Safety Research Consortium: can the thorough QT/QTc study be replaced by early QT assessment in routine clinical pharmacology studies? Scientific update and a research proposal for a path forward. *Am Heart J* 168:262–272
- Denac H, Mevisen M, Scholtysik G (2000) Structure, function and pharmacology of voltage-gated sodium channels. *Naunyn Schmiedebergs Arch Pharmacol* 362:453–479
- DePonti F, Poluzzi E, Cavalli A, Recanatini M, Montanaro N (2002) Safety of non-antiarrhythmic drugs that prolong the QT interval or induce torsade de pointes: an overview. *Drug Saf* 25:263–286
- DeWaard M, Pragnel M, Campbell KP (1994) Ca<sup>2+</sup> channel regulation by a conserved beta subunit domain. *Neuron* 13:495–503
- DiFrancesco D, Noble D (1985) A model of cardiac electrical activity incorporating ionic pumps and concentration changes. *Philos Trans R Soc Lond* 307:353–398
- Einthoven WE (1912) The different forms of the human electrocardiogram and their signification. *Lancet* 1:853–861
- Ertel EA, Campbell KP, Harpold MM, Hofmann F, Mori Y et al (2000) Nomenclature of voltage-gated calcium channels. *Neuron* 25:533–535
- Farkas A, Coker SJ (2002) Limited induction of torsade de pointes by terikalant and erythromycin in an in vivo model. *Eur J Pharmacol* 449:143–153
- Gibson JK, Bronson J, Palmer C, Numann R (2014) Adult human stem cell-derived cardiomyocytes detect drug-mediated changes on action potentials. *J Pharmacol Toxicol Methods* 70:255–267
- Gintant GA (1995) Regional differences in IK density in canine left ventricle: role of IKs in electrical heterogeneity. *Am J Physiol* 268:H604–H613
- Goineau S, Castagné V, Guillaume P, Froget G (2012) The comparative sensitivity of three in vitro safety pharmacology models for the detection of lidocaine-induced cardiac effects. *J Pharmacol Toxicol Methods* 66:52–58
- Goldin AL (1993) Accessory subunits and sodium channel inactivation. *Curr Opin Neurobiol* 3:272–277
- Goldin AL (2001) Resurgence of sodium channel research. *Annu Rev Physiol* 63:871–894
- Grandi E, Pasqualini FS, Bers DM (2010) A novel computational model of the human ventricular action potential and Ca transient. *J Mol Cell Cardiol* 48:112–121
- Guo W, Li H, London B, Nerbonne JM (2000) Functional consequences of elimination of *i*(to, f) and *i*(to, s): early afterdepolarizations, atrioventricular block, and ventricular arrhythmias in mice lacking Kv1.4 and expressing a dominant-negative Kv4 alpha subunit. *Circ Res* 87:73–79
- Guo L, Dong Z, Guthrie H (2009) Validation of a guinea pig Langendorff heart model for assessing potential cardiovascular liability of drug candidates. *J Pharmacol Toxicol Methods* 60:130–151
- Gussak I, Chaitman BR, Kopecky SL, Nerbonne JM (2000) Rapid ventricular repolarization in rodents: electrocardiographic manifestations, molecular mechanisms, and clinical insights. *J Electrocardiol* 33:159–170

- Hamlin RL, Cruze CA, Mittelstadt SW, Kijawornrat A, Keene BW, Roche BM, Nakayama T, Nakayama H, Hamlin DM, Arnold T (2004) Sensitivity and specificity of isolated perfused guinea pig heart to test for drug-induced lengthening of QTc. *J Pharmacol Toxicol Methods* 49:15–23
- Han W, Wang Z, Nattel S (2000) A comparison of transient outward currents in canine cardiac Purkinje cells and ventricular myocytes. *Am J Physiol* 279:H466–H474
- Hanck DA, Makielski JC, Sheets MF (1994) Kinetic effects of quaternary lidocaine block of cardiac sodium channels: a gating current study. *J Gen Physiol* 103:19–43
- Hanson LA, Bass AS, Gintant G, Mittelstadt S, Rampe D, Thomas K (2006) ILSI-HESI cardiovascular safety subcommittee initiative: evaluation of three non-clinical models of QT prolongation. *J Pharmacol Toxicol Methods* 54:116–129
- Hill JL, Gettes LS (1980) Effect of acute coronary artery occlusion on local myocardial extracellular K<sup>+</sup> activity in swine. *Circulation* 61:769–778
- Hille B (1992) Ionic channels of excitable membranes. Sinauer Associates, Sunderland
- Hodgkin AL, Huxley AF (1952) A quantitative description of membrane current and its application to conduction and excitation in nerve. *J Physiol* 116:500–544
- Hondeghem LM (1994) Computer aided development of antiarrhythmic agents with class IIIa properties. *J Cardiovasc Electrophysiol* 5:711–721
- Hondeghem LM, Hoffmann P (2003) Blinded test in isolated female rabbit heart reliably identifies action potential duration prolongation and proarrhythmic drugs: importance of triangulation, reverse use dependence, and instability. *J Cardiovasc Pharmacol* 41:14–24
- Hondeghem LM, Katzung BG (1977) Time- and voltage-dependent interactions of antiarrhythmic drugs with cardiac sodium channels. *Biochim Biophys Acta* 472:373–398
- Hoppe UC, Marban E, Johns DC (2001) Distinct gene-specific mechanisms of arrhythmia revealed by cardiac gene transfer of two long QT disease genes, HERG and KCNE1. *Proc Natl Acad Sci USA* 98:5335–5340
- Hubbard JI, Llinas R, Quastel DMJ (1969) Electrophysiological analysis of synaptic transmission. Edward Arnold, London
- Isom LL, De Jongh KS, Patton DE, Reber BF, Offord J, Charbonneau H, Walsh K, Goldin AL, Catterall WA (1992) Primary structure and functional expression of the beta 1 subunit of the rat brain sodium channel. *Science* 256:839–842
- Jahnel U, Klemm P, Nawrath H (1994) Different mechanisms of the inhibition of the transient outward current in rat ventricular myocytes. *Naunyn Schmiedeberg Arch Pharmacol* 349:87–94
- Ju YK, Saint DA, Gage PW (1992) Effects of lignocaine and quinidine on the persistent sodium current in rat ventricular myocytes. *Br J Pharmacol* 107:311–316
- Khodorov B, Shishkova L, Peganov E, Revenko S (1976) Inhibition of sodium currents in frog Ranvier node treated with local anesthetics. Role of slow sodium inactivation. *Biochim Biophys Acta* 433:409–435
- Kirsch GE, Trepakova ES, Brimecombe JC, Sidach SS, Erickson HD, Kochan MC, Shyja LM, Lacerda AE, Brown AM (2004) Variability in the measurement of hERG potassium channel inhibition: effects of temperature and stimulus pattern. *J Pharmacol Toxicol Methods* 50:93–101
- Klugbauer N, Lacinova L, Marais E, Hobom M, Hofmann F (1999) Molecular diversity of the calcium channel alpha2delta subunit. *J Neurosci* 19:684–691
- Kuryshv YA, Wible BA, Gudz TI, Ramirez AN, Brown AM (2001) KChAP/Kvbeta1.2 interactions and their effects on cardiac Kv channel expression. *Am J Physiol Cell Physiol* 281:C290–C299
- Kwak YG, Navarro-Polanco RA, Grobaski T, Gallagher DJ, Tamkunk MM (1999) Phosphorylation is required for alteration of kv1.5K(+) channel function by the Kvbeta1.3 subunit. *J Biol Chem* 274:25355–25361

- Lawrence CL, Bridgland-Taylor MH, Pollard CE, Hammond TG, Valentin J-P (2006) A rabbit Langendorff heart proarrhythmia model: predictive value for clinical identification of Torsades de Pointes. *Br J Pharmacol* 149:845–860
- Lee N, Authier S, Pugsley MK, Curtis MJ (2010) The continuing evolution of torsades de pointes liability testing methods: is there an end in sight? *Toxicol Appl Pharmacol* 243:146–153
- Li H, Fuentes-Garcia J, Towbin JA (2000) Current concepts in long QT syndrome. *Pediatr Cardiol* 21:542–550
- Lindgren S, Bass AS, Briscoe R, Bruse K, Friedrichs GS, Kallman M-J, Markgraf C, Patmore L, Pugsley MK (2008) Benchmarking safety pharmacology regulatory packages and best practice. *J Pharmacol Toxicol Methods* 58:99–109
- Liu T, Brown BS, Wu Y, Antzelevitch C, Kowey PR, Yan GX (2006) Blinded validation of the isolated arterially perfused rabbit ventricular wedge in preclinical assessment of drug-induced proarrhythmias. *Heart Rhythm* 3:948–956
- Lu HR, Mariën R, Saels A, De Clerck F (2000) Are there sex-specific differences in ventricular repolarization or in drug-induced early afterdepolarizations in isolated rabbit Purkinje fibers? *J Cardiovasc Pharmacol* 36:132–139
- Lu HR, Mariën R, Saels A, De Clerck F (2001) Species plays an important role in drug-induced prolongation of action potential duration and early afterdepolarizations in isolated Purkinje fibers. *J Cardiovasc Electrophysiol* 12:93–102
- Lu HR, Vlamincx E, Gallacher DJ (2008) Choice of cardiac tissue in vitro plays an important role in assessing the risk of drug-induced cardiac arrhythmias in human: beyond QT prolongation. *J Pharmacol Toxicol Methods* 57:1–8
- Luo C, Rudy Y (1991) A model of the ventricular action potential: depolarization, repolarization, and their interaction. *Circ Res* 68:1501–1526
- MacKinnon R, Cohen SL, Kuo A, Lee A, Chait BT (1998) Structural conservation in prokaryotic and eukaryotic potassium channels. *Science* 280:106–109
- Main MC, Bryant SM, Hart G (1998) Regional differences in action potential characteristics and membrane currents of guinea-pig left ventricular myocytes. *Exp Physiol* 83:747–761
- Malik M, Camm AJ (2001) Evaluation of drug-induced QT Interval prolongation: implications for drug approval and labelling. *Drug Saf* 24:323–351
- Mirams GR, Davies MR, Brough SJ, Cui Y, Gavaghan DJ, Abi-Gerges N (2014) Prediction of thorough QT study results using action potential simulations based on ion channel screens. *J Pharmacol Toxicol Methods* 70:246–254
- Nakamura TY, Coetzee WA, Vega-Saenz De Miera E, Artman M, Rudy B (1997) Modulation of Kv4 channels, key components of rat ventricular transient outward K<sup>+</sup> current by PKC. *Am J Physiol* 273:H1775–H1786
- Nalos L, Varkevisser R, Jonsson MK, Houtman MJ, Beekman JD et al (2012) Comparison of the IKr blockers moxifloxacin, dofetilide and E-4031 in five screening models of pro-arrhythmia reveals lack of specificity of isolated cardiomyocytes. *Br J Pharmacol* 165:467–478
- Nerbonne JM (2000) Molecular basis of functional voltage-gated K<sup>+</sup> channel diversity in the mammalian myocardium. *J Physiol* 525:285–298
- O'Hara T, Virág L, Varró A, Rudy Y (2011) Simulation of the undiseased human cardiac ventricular action potential: model formulation and experimental validation. *PLoS Comput Biol* 7(5):e1002061. doi:10.1371/journal.pcbi.1002061
- Pawson AJ, Sharman JL, Benson HE, Faccenda E, Alexander SP, Buneman OP, Davenport AP, McGrath JC, Peters JA, Southan C, Spedding M, Yu W, Harmar AJ, NC-IUPHAR (2014) The IUPHAR/BPS Guide to PHARMACOLOGY: an expert-driven knowledgebase of drug targets and their ligands. *Nucleic Acids Res* 42:D1098–D1106
- Peng S, Lacerda AE, Kirsch GE, Brown AM, Bruening-Wright A (2010) The action potential and comparative pharmacology of stem cell-derived human cardiomyocytes. *J Pharmacol Toxicol Methods* 61:277–286

- Puddu PE, Legrand J-C, Sallé L, Rouet R, Ducroq J (2011) I(Kr) vs. I(Ks) blockade and arrhythmogenicity in normoxic rabbit Purkinje fibers: does it really make a difference? *Fundam Clin Pharmacol* 25:304–312
- Pugsley MK (2002) Antiarrhythmic drug development: historical review and future perspective. *Drug Dev Res* 55:3–16
- Pugsley MK, Quastel DMJ (1998) Basic cardiac electrophysiology. In: Pugsley MK, Walker MJA (eds) *Methods in cardiac electrophysiology*. CRC Press, Boca Raton, FL
- Pugsley MK, Authier S, Curtis MJ (2008) Principles of safety pharmacology. *Br J Pharmacol* 154:1382–1399
- Pugsley MK, Dalton JA, Authier S, Curtis MJ (2014) Safety pharmacology in 2014: new focus on non-cardiac methods and models. *J Pharmacol Toxicol Methods* 70:170–174
- Ragsdale DS, McPhee JC, Scheuer T, Catterall WA (1996) Common molecular determinants of local anesthetic, antiarrhythmic, and anticonvulsant block of voltage-gated Na<sup>+</sup> channels. *Proc Natl Acad Sci USA* 93:9270–9275
- Rasmusson RL, Morales MJ, Wang S, Liu S, Campbell DL, Brahmajothi MV, Strauss HC (1998) Inactivation of voltage-gated cardiac K<sup>+</sup> channels. *Circ Res* 82:739–750
- Rees SA, Curtis MJ (1995) Further investigations into the mechanism of antifibrillatory action of the specific IK1 blocker, RP58866, assessed using the rat dual coronary perfusion model. *J Mol Cell Cardiol* 27:2595–2606
- Roberts R, Brugada R (2000) Genetic aspects of arrhythmias. *Am J Med Genet* 97:310–318
- Rolf S, Haverkamp W, Borggreffe M, Musshoff U, Eckardt L, Mergenthaler J et al (2000) Effects of antiarrhythmic drugs on cloned cardiac voltage-gated potassium channels expressed in *Xenopus* oocytes. *Naunyn Schmiedebergs Arch Pharmacol* 362:22–31
- Roy M, Dumaine R, Brown AM (1996) HERG, a primary human ventricular target of the non-sedating antihistamine terfenadine. *Circulation* 94:817–823
- Sager PT, Gintant G, Turner JR, Pettit S, Stockbridge N (2014) Rechanneling the cardiac proarrhythmia safety paradigm: a meeting report from the Cardiac Safety Research Consortium. *Am Heart J* 167:292–300
- Saint DA (2007) The cardiac persistent sodium current: an appealing therapeutic target? *Br J Pharmacol* 153:1133–1142
- Saint DA, Ju YK, Gage PW (1992) A persistent sodium current in rat ventricular myocytes. *J Physiol* 453:219–231
- Sakura H, Bond C, Warren-Perry M, Horsley S, Kearney L, Tucker S, Adelman J, Turner R, Ashcroft FM (1995) Characterization and variation of a human inwardly-rectifying-K-channel gene (KCNJ6): a putative ATP-sensitive K-channel subunit. *FEBS Lett* 367:193–197
- Sanguinetti MC, Jurkiewicz NK (1991) Delayed rectifier outward K<sup>+</sup> current is composed of two currents in guinea pig atrial cells. *Am J Physiol* 260:H393–H399
- Sato C, Ueno Y, Asai K, Takahashi K, Sato M, Engel A, Fujiyoshi Y (2001) The voltage-sensitive sodium channel is a bell-shaped molecule with several cavities. *Nature* 409:1047–1051
- Schaper W, Schaper J, Winkler B (1986) The collateral circulation of the heart. *J Mol Cell Cardiol* 18:60
- Sedmera D, Gourdie RG (2014) Why do we have Purkinje fibers deep in our heart? *Physiol Res* 63: S9–S18
- Shah RR (2001) Drug-induced prolongation of the QT interval: why the regulatory concern? *Fundam Clin Pharmacol* 16:119–124
- Snyders DJ (1999) Structure and function of cardiac potassium channels. *Cardiovasc Res* 42:377–390
- Striessnig J (1999) Pharmacology, structure and function of cardiac L-type Ca<sup>2+</sup> channels. *Cell Physiol Biochem* 9:242–269
- Studenik CR, Zhou Z, January C (2001) Differences in action potential and early afterdepolarization properties in LQT2 and LQT3 models of long QT syndrome. *Br J Pharmacol* 132:85–92

- Tanaka T, Tohyama S, Murata M, Nomura F, Kaneko T, Chen H, Hattori F, Egashira T, Seki T et al (2009) In vitro pharmacologic testing using human induced pluripotent stem cell-derived cardiomyocytes. *Biochem Biophys Res Commun* 385:497–502
- ten Tusscher KH, Panfilov AV (2006) Cell model for efficient simulation of wave propagation in human ventricular tissue under normal and pathological conditions. *Phys Med Biol* 51:6141–6156
- Topert C, Doring F, Derst C, Daut J, Grzeschik KH, Karschin A (2000) Cloning, structure and assignment to chromosome 19q13 of the human Kir2.4 inwardly rectifying potassium channel gene (KCNJ14). *Mamm Genome* 11:247–249
- Vaughan Williams EM (1984) A classification of antiarrhythmic actions reassessed after a decade of new drugs. *J Clin Pharmacol* 24:129–147
- Vidarsson H, Hyllner J, Sartipy P (2010) Differentiation of human embryonic stem cells to cardiomyocytes for in vitro and in vivo applications. *Stem Cell Rev* 6:108–120
- Vos MA (2001) Preclinical evaluation of antiarrhythmic drugs: new drugs should be safe to be successful. *J Cardiovasc Electrophysiol* 12:1034–1036
- Wang G, Dugas M, Ben Armah I, Honerjager P (1990) Interaction between DPI 201-106 enantiomers at the cardiac sodium channel. *Mol Pharmacol* 37:17–24
- Wang Z, Yue L, White M, Pelletier G, Nattel S (1998) Differential distribution of inward rectifier potassium channel transcripts in human atrium versus ventricle. *Circulation* 98:2422–2428
- Wang D, Patel C, Cui C, Yan GX (2008) Preclinical assessment of drug-induced proarrhythmias: Role of the arterially perfused rabbit left ventricular wedge preparation. *Pharmacol Ther* 119:141–151
- Weiss JN, Venkatesh N (1993) Metabolic regulation of cardiac ATP-sensitive K<sup>+</sup> channels. *Cardiovasc Drugs Ther* 7:499–505
- West JW, Patton DE, Scheuer T, Wang Y, Goldin AL, Catterall WA (1992) A cluster of hydrophobic amino acid residues required for fast Na<sup>(+)</sup>-channel inactivation. *Proc Natl Acad Sci U S A* 89:10910–10914
- Wickenden AD, Jegla TJ, Kaprielian R, Backx PH (1999) Regional contributions of Kv1.4, Kv4.2, and Kv4.3 to transient outward K<sup>+</sup> current in rat ventricle. *Am J Physiol* 276:H1599–H1607
- Williams BA, Dickenson DR, Beatch GN (1999) Kinetics of rate-dependent shortening of action potential duration in guinea-pig ventricle; effects of IK1 and IKr blockade. *Br J Pharmacol* 126:1426–1436
- Wit AL, Rosen MR (1983) Pathophysiologic mechanisms of cardiac arrhythmias. *Am Heart J* 106:798–811
- Wu MH, Su MJ, Sun SS (1999) Electrophysiological profile after inward rectifier K channel blockade by barium in isolated rabbit hearts. Altered repolarization and unmasked decremental conduction property. *Europace* 1:85–95
- Xu H, Guo W, Nerbonne JM (1999) Four kinetically distinct depolarization-activated K<sup>+</sup> currents in adult mouse ventricular myocytes. *J Gen Physiol* 113:661–678
- Yan GX, Antzelevitch C (1996) Cellular basis for the electrocardiographic J wave. *Circulation* 93:372–379
- Yan GX, Antzelevitch C (1998) Cellular basis for the normal T wave and the electrocardiographic manifestations of the long QT syndrome. *Circulation* 98:1928–1936
- Yan GX, Shimizu W, Antzelevitch C (1998) Characteristics and distribution of M cells in arterially perfused canine left ventricular wedge preparations. *Circulation* 98:1921–1927
- Yang T, Roden DM (1996) Extracellular potassium modulation of drug block of IKr. Implications for torsade de pointes and reverse use-dependence. *Circulation* 93:407–411
- Yue L, Feng J, Gaspo R, Li GR, Wang Z, Nattel S (1997) Ionic remodeling underlying action potential changes in a canine model of atrial fibrillation. *Circ Res* 81:512–525
- Yue L, Feng J, Wang Z, Nattel S (1999) Adrenergic control of the ultrarapid delayed rectifier current in canine atrial myocytes. *J Physiol* 516:385–398
- Zaza A, Belardinelli L, Shryock JC (2008) Pathophysiology and pharmacology of the cardiac “late sodium current”. *Pharmacol Ther* 119:326–339